$E0$, $E1$, $E2$, $E3$, and $E4$ giant resonances in the $N = 82$ nucleus ^{140}Ce between 4 and 48 MeV excitation energy with inelastic electron scattering

R. Pitthan, H. Hass, D. H. Meyer, F. R. Buskirk, and J. N. Dyer
Department of Physics and Chemistry, Naval Postgraduate School, Monterey, California 93940
(Received 18 September 1978)

The cross section for electron scattering from natural cerium (89% ^{140}Ce) has been measured with electrons of 80 and 92 MeV at 90 and 105° between 4 and 48 MeV excitation energy. The nine resonances or resonance-like structures identified at E_x = 6 (31 $A^{-1/3}$), 7.4 (38 $A^{-1/3}$), 10 (52 $A^{-1/3}$), 12 (62 $A^{-1/3}$), 15.3 (79 $A^{-1/3}$), 22 (114 $A^{-1/3}$), 25 (130 $A^{-1/3}$), 31 (160 $A^{-1/3}$), and 37.5 (195 $A^{-1/3}$) MeV were classified on the basis of their momentum transfer dependence and discussed in the framework of the shell model. Since some of the arguments used are intricate we refer for quantitative particulars to the text. It is shown that the $E2$ sum rule strength not exhausted in the excitation range of this experiment may contribute up to 50% of the classical dipole sum rule to the photon cross section between 50 MeV and the pion threshold. The resonance at 10 MeV might be due to a separate oscillation of the excess neutrons against the rest of the nucleus.

[NUCLEAR REACTIONS ^{140}Ce(e,e'), E_0 = 50 to 92 MeV, Measured $d^2\sigma/d\Omega dE_x$, bound and continuum states (giant resonances). Deduced multipolarity, reduced matrix element $B(E\lambda)$, radiative width Γ_γ°, sum rule exhaustion of giant resonances, photon cross section to pion threshold, total width of continuum and clustered states.]

I. INTRODUCTION

Recent years have brought a vastly improved knowledge of the nuclear giant resonances,[1] which are broadly defined as coherent nuclear excitations above the lowest particle threshold. However, as many or more questions have arisen as have been solved. The particular target of this work (^{nat}Ce which contains 89% ^{140}Ce) had been chosen for several reasons which we thought made it a particularly interesting and worthwhile nucleus to study. First, the earliest work on giant multipole resonances[2] pointed out several problems with the giant dipole resonance in $N = 82$ nuclei, which do not fit the normal characterization of this state as well understood, and will be discussed in Sec. IV B. Secondly, a resonance at $53A^{-1/3}$ MeV, also discovered[3] in ^{140}Ce and seen in many nuclei by subsequent (e,e') measurements exhibits an $E2$ angular distribution (or momentum transfer dependence). The presence of a second separate $E2$ branch in addition to the main isoscalar giant quadrupole resonance (GQR) at $63A^{-1/3}$ MeV, which already carries between 50 and 100% of the isoscalar sum rule in heavy nuclei, is difficult to understand. Thirdly, resonances reported above 25 to 30 MeV, that is above the isovector GQR at $130A^{-1/3}$ MeV,[4] have been found in five nuclei heavier than ^{140}Ce and have been classified alternatively as $E0$ or $E3$ and, in fact, may contain both multipolarities. Lastly, a general reason to choose ^{140}Ce is based on the observation that $N = 82$ nuclei have one of the most favorable ratios of width of the various GR to their energy separation. Since the overlapping of the giant resonances of different multipolarity poses the largest problem in interpretation of observed electro-excitation spectra, the small intrinsic width of the resonances in Ce is of great help in unraveling the complicated structure with a line shape fit.

Giant electric quadrupole resonances have been found to have properties which only slowly vary from nucleus to nucleus and to be not much different in magic and nonmagic (especially deformed) nuclei, a property which is understood in the framework of the shell model.[5] Other resonances like the $E3$ have been found to show more variance, but have still to be looked at in conjunction with measurements over a wide range of A. We will, therefore, shortly describe the general theoretical framework.

Despite early predictions of a hydrodynamical $E2$ mode in analogy to the $E1$,[6] the giant multipole resonance region experimentally was found to be flat until 1971. None of the "eagerly expected high-frequency collective modes"[7] could be found. The theoretical foundation for a microscopic understanding of the GMR region had been laid two decades ago by Brown *et al.*[8]; the most detailed predictions had been given by Bohr and Mottelson[9] within their self-consistent shell model. One of the best short descriptions of the scheme proposed by Bohr and Mottelson has been given by Hamamoto[10]; results based on a RPA calculation are summarized in Table I and can be explained in the following way in terms of the nuclear shell model. Without taking isospin into account, a GR

TABLE I. Random phase approximation (RPA) calculations of Hamamoto (Ref. 10) for the principal main shell transitions into the continuum. While this simple model naturally can not account for finer details, like the fine structure found in ^{208}Pb (Ref. 32), it describes the giant resonances found to date very well. A different approach by Suski (Ref. 94) based on sum rule considerations predicts in addition the monopole strength to be located at 58 and 178 $A^{-1/3}$ MeV for the isoscalar and isovector part, respectively.

λ	$\hbar\omega_0$ [a]	E_X ($A^{-1/3}$ MeV)	R [b] (%)	E_X ($A^{-1/3}$ MeV)	R (%)
2	2	58	100	135	100
3	1	25	28	53	2
	3	107	72	197	98
4	2	62	51	107	3
	4	152	49	275	97

[a] $\hbar\omega_0 = 41A^{-1/3}$ MeV.
[b] $R = E_X B(E\lambda, q=0)/\mathrm{EWSR}(E\lambda, \Delta T)\times 100$.

of a certain multipolarity would be found at an excitation energy corresponding to a number of main shell transitions ($\hbar\omega_0 = 41A^{-1/3}$ MeV) allowed by spin and parity, i.e., $2\hbar\omega_0$ for $E2$, $1\hbar\omega_0$ and $3\hbar\omega_0$ for $E3$, etc. The isospin dependence of the particle-hole interaction, repulsive for isovector excitations, [8] attractive for isoscalar ones, introduces another degree of freedom. The unperturbed state, i.e., $80A^{-1/3}$ MeV for an $E2$, is thus split in two, with the isoscalar part ($\Delta T = 0$) lowered to $\approx 60A^{-1/3}$ MeV and the isovector part ($\Delta T = 1$) raised to $\approx 130A^{-1/3}$ MeV.[11] Figure 1 shows most of the available body of data from inelastic electron scattering[12] for multipolarities $\lambda \geq 1$. If one compares with Table I, in general, a good agreement between schematic model and experiment is obvious. The most complete experimental survey of any mode has been made with (α, α') by Youngblood *et al.* for the isoscalar GQR, [13] and for the $1\hbar\omega$, $\Delta T = 0$ high energy bound octupole state (HEBOS), [14] predicted early by Bohr and Mottelson, [9] at $32A^{-1/3}$ MeV.

II. EXPERIMENTAL DETAILS

The experiment reported here used electrons of primary energy (80 and 92 MeV) at angles of 90 and 105°, from the 120 MeV electron Linac of the Naval Postgraduate School, the combination being a compromise between the goals of keeping the transverse contribution small (forward angle) but having large cross sections (E_0 small). The forward angle (93°) measurements of Ref. 2 with 50 and 65 MeV electrons were included in the analysis because they fulfill these conditions. The momentum transfer thus covered the range from 0.37 fm^{-1} to 0.75 fm^{-1} for zero excitation energy. ^{nat}Ce metal (89% ^{140}Ce) from Ventron Corporation was rolled into self-supporting targets with a mass density of 126 mg/cm^2 (corresponding to 1.58% radiation length[15]). The inelastic data were measured relative to the elastic cross section, thus eliminating systematic uncertainties arising from determination of solid angle, counter efficiencies, charge integration, etc. The elastic cross section σ_{el} was calculated with the phase shift code of Fischer and Rawitscher, [16] using c, t values for the charge distribution of the ground state from muonic atoms, $c = 5.78$ and $t = 2.31$ fm^2.

The experimental setup of the NPS Linac has been described recently[16] and is here only summarized for sake of completeness. The accelerated electrons are momentum analyzed in the symmetry plane of a two 30° sector magnet achromatic deflection system. The electrons scattered from the target are measured by a ten scintillation counter ladder in the focal plane of a 40 cm, 120° double focusing magnetic spectrometer. The momentum bite of the spectrometer is 3%, the stepping width of the magnetic field normally corresponds to 0.1 MeV. The overall resolution of the system is limited by the mechanical dimensions of the scintillators and, therefore, maximally 0.3%. It was kept to 0.5%, however, because this value is the optimal compromise between background produced at the energy defining slit system, which rises with better resolution, i.e., narrower slits, and background produced in the beam pipes leading to the spectrometer, which rises with wider slits. The data are sorted into energy bins equal to the stepping width (0.1 MeV). Typical spectra are shown in Figs. 2 and 3. For control purposes the whole excitation range has been measured with a wider stepping width, 2 MeV, before and after each inelastic run. No deviations, indicative of background changes, integrator drifts, etc., were found. The spectrum with the highest momentum transfer, 92 MeV at 105°, was measured twice to achieve a good statistical accuracy. Each run took approximately 100 hours of beam time.

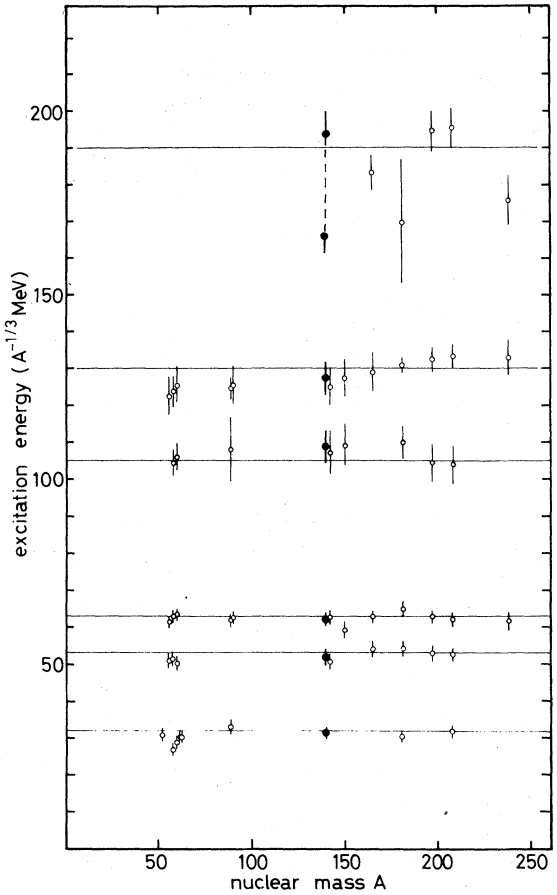

FIG. 1. Excitation energy of resonant cross section above approximately $30A^{-1/3}$ MeV as a function of A. The lines have been drawn solely to guide the eye. Although this plot does not enable one to decide on the multipolarity of the states found, certain systematic features are apparent. Excitation energies seem to be fairly constant for resonances at ~30, 63, and $105A^{-1/3}$ MeV, but drop distinctly over the range of A covered for the resonances grouped around $130A^{-1/3}$ MeV. Since this behavior is reminiscent of the GDR, an isovector state, and since the $130A^{-1/3}$ MeV state has also been identified as isovector ($E2$), one may conclude that isovector states fall off in excitation energy with A, while isoscalar rates do not, at least between $A \approx 50$ and 208. Some irregular features, concerning the 53 and $\sim 190A^{-1/3}$ MeV states are discussed in the text. Only results from (e, e') are shown. Not presented is the GDR because its energy is much better known from (γ, n) results (Ref. 61).

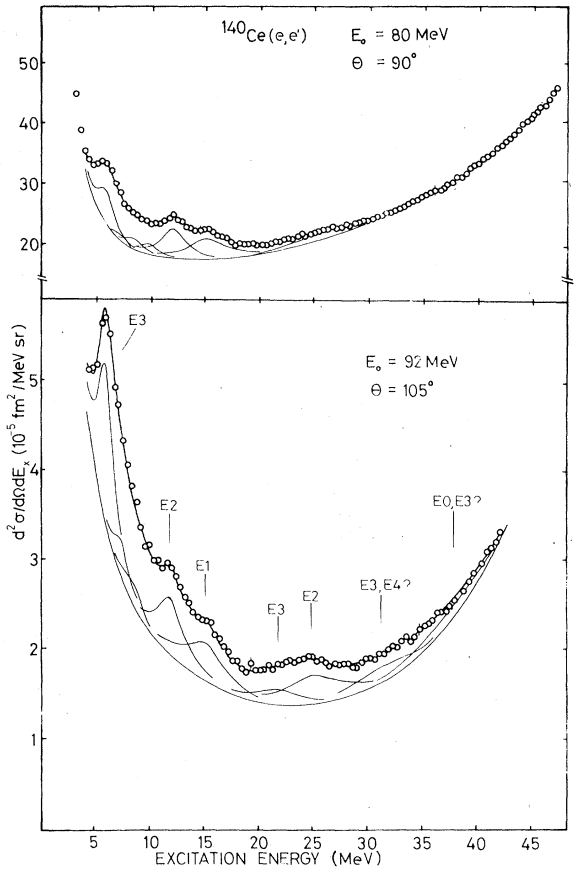

FIG. 2. Spectra of 80 and 92 MeV electrons scattered inelastically from ^{140}Ce. Resonances (or envelopes of discrete states) are indicated and discussed in more detail in the text. The bottom curved line in both parts is the fitted total background. Note that zero in the lower spectrum is *not* suppressed. The ghost peak has not been subtracted from the data, neither are the cross sections corrected for the constant dispersion of the magnetic spectrometer. The spectra were taken and fitted with 10 points per MeV, which were reduced for graphical purposes by a factor of 4. Resolution was 500 keV, approximately $\frac{1}{3}$ of the width of the smallest resonance found; the statistical error is shown on selected points in the lower spectrum; it was smaller than the circles in the upper one. The fitted range of the spectra shown was 4–48 MeV for the upper, and 4–42 MeV for the lower spectrum (see discussion in text in conjunction with the 37 MeV state).

III. EVALUATION

A. Background

The general principles of evaluation have been described recently including the various types of background (radiative, general room, target-in) which have to be determined, background function, χ^2 tests, reduced transition probabilities, and sum rules. We refer to Sec. III of Ref. 16 for particulars. The radial integrals $\langle r^{2k} \rangle$ needed for the evaluation of the sum rules can be calculated from the c, t values by

$$\langle r^k \rangle = c^k/(2k+6)\{6 + (k^2+5k)[\pi t/(4t \ln 3)]^2\}.$$

Our choice for the line shape used for the fit of the strength function (Breit-Wigner) is based on a

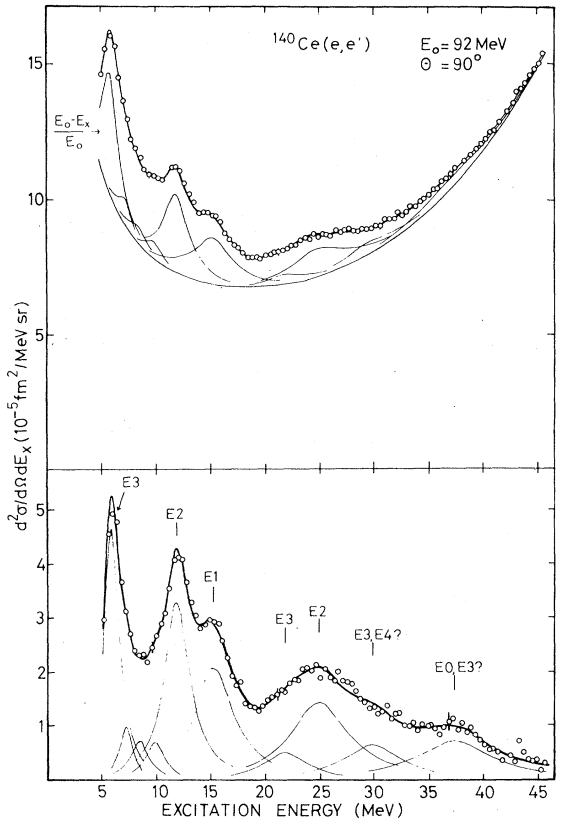

FIG. 3. Spectrum of 92.1 MeV electrons scattered inelastically from ^{140}Ce at 90°. The spectrum with and without the background is shown together so that the difference between the two may be seen. The resonances which were used for fitting the spectrum and the background as described in the text are drawn. The "ghost peak" is not subtracted from the upper graph. The spectrum was taken and fitted with 10 data points per MeV. For graphical purposes the number of points for the spectrum was reduced by a factor of 4. The fitting range was 4–48 MeV. The statistical error is shown on selected points. While the upper part has not been corrected for the constant dispersion of the magnetic spectrometer and thus shows the data points as measured, the subtracted spectrum has been corrected, in order to show the cross sections of the resonances in their true relation.

recent investigation of the line shape of the GDR.[17] Although line shapes for resonances of different multipolarity could differ in principle, it seems unlikely. In any case, using a Lorentz form would not change the results outside the error assigned.

In deviation from earlier procedure[16] we have, however, tried various background forms. The smallest χ^2 was achieved with

$$\mathrm{BGR4}(E_f) = P_1 + P_2/E_f + P_3 T_R \exp[P_4(E_i - E_f)/E_f];$$

but $\mathrm{BGR3}(E_f) = P_1 + P_2/E_f + P_3 E_f + T_R$ did nearly as well. The simplest form for BGR which still described the data reasonably well and produced an acceptable χ^2 was

$$\mathrm{BGR2}(E_f) = P_1 + P_2/E_f + T_R .$$

(E_i = elastic energy, E_f = energy of the scattered electron, P_i fitted parameters, T_R calculated radiation tail, see below). Other forms used were of the type BGR2 or BGR4 with just more terms P_n/E_f^{n-1} or $P_n E_f^{n-1}$ added. Such terms did not improve the fit.

Naively, one would identify in BGR2 the P_1 term with the constant room background and the P_2/E_f term as a corrective term for the failure of the radiation tail calculation at higher excitation energies. However, the terms are not what they seem to be, a confusion which arises from the effects of the constant dispersion of the magnetic spectrometer. Since the momentum bite becomes smaller with smaller magnetic field (E_f), the actual count rates are lower by E_f/E_i and the spectra have to be dispersion corrected. Quite naturally one takes the elastic energy E_i as reference point and multiplies the count rates with E_i/E_f.

Since some of the components which contribute to the total background undergo the dispersion and others do not, a closer look into what happens is necessary. 1. The general room background (GRB) is defined as the electrons which penetrate the counter shielding. Since they do not travel through the spectrometer, they are not affected by the dispersion. As an approximation for GRB we use the count rate 10 MeV above the elastic peak. This value is subtracted from the total spectrum (elastic and inelastic) before any other data handling. Any leftover, due to errors in the determination of GBR, would contribute to BRG in the form of a constant term P_1. 2. That part of BGR that comes through the spectrometer (SB) undergoes dispersion. Two assumptions about the nature of this background are possible: (a) SB fills the spectrometer evenly with electrons, if the spectrometer setting is far enough from the elastic peak. In this case it would contribute to P_1. (b) SB is produced by the elastic peak, when it hits the walls of the spectrometer. In this case it will either produce the ghost peak, care of which is taken through the simultaneous fitting of an empirically shaped ghost peak line in the immediate vicinity of the ghost peak at 92% of the elastic energy. A more constant part of the experimental scattering would fall off with E_f, because the elastic electrons will hit further and further away from the counters. For this latter part we assume the lowest order ansatz $P_2 E_f$. 3. The radiation tail (T_R) events come through the spectrometer and have undergone dispersion, but

they are trivial to treat because of $T_{R,\text{exp}} = T_{R,\text{true}} \times E_f/E_i$. Since in the analysis the step after subtraction of GBR (as measured 10 MeV above the elastic peak) is the dispersion correction E_i/E_f, we have the following (E_i constant) relations:

$$P_1 \to P_1 E_i/E_f \to P_1'/E_f ,$$

$$P_2 E_f \to P_2' E_i \to P_2'' .$$

If we rename $P_1' \to P_2'$ and $P_2'' \to P_1$, we end up with BGR2.

In addition we have, in a heuristic manner, to take care of the divergence between calculated and measured radiation tail. We know from experiment that the difference $T_{R,D} = T_{R,\text{exp}} - T_{R,\text{calc}}$ rises with excitation energy E_x. Since $E_x \approx E_i - E_f$, we have the lowest order ansatz possible, $P_1 + P_2 E_x = P_1 + P_2' E_f$. Again, after dispersion correction this does not change the functional form of BGR2; only P_1 and P_2 have a more complicated meaning. It can easily be shown that BGR3 would correspond to a second order Taylor series for $T_{R,D}$. BGR4 was originally tried, because we did not know the order required to fit the difference. In this case it is always advisable to try an exponential ansatz as in BGR4, because in principle it contains all orders. The special form of BGR4 comes from the boundary conditions imposed, namely $T_{R,D} = 0$ for $E_i = E_f$ (by definition) and $T_{R,D} = \infty$ for $E_f \to 0$.

If we express P_1 and P_2 in fractions of the minimum of the radiation tail, typical values for the fit parameters for BGR4 are $P_1 = 0.30 \pm 0.02$, $P_2 = 0.01 \pm 0.01$ (this term characterizes mainly the accidentals), $P_3 = (0.95 \text{ to } 1.05) \pm 0.03$, and $P_4 = +0.25 \pm 0.05$. It is important to note that P_2, P_3, and P_4 are highly correlated with correlation factors in the range 0.7 to 0.9. This explains why BGR2 does still do a good job when compared to the more complicated BGR4.

B. Errors

The error assignment to giant resonance cross sections is sometimes difficult. Since many variables enter, the purely statistical error is mostly too small. Most recent hadron scattering experiments seem to apply an overall 20% error to their final results (see, e.g., Refs. 18 and 19), while typical errors in (e, e') are on the 10% level for the major resonances.[16,20,21] The (e, e') errors are presumably smaller because there are fewer systematic errors due to the measurement relative to the elastic peak, and the background is known, at least in principle, while inelastic hadron scattering experiments have to work with a totally heuristic background.

The errors quoted in this paper are based on the statistical error for the excitation energy, and on two times the statistical error for half-width and B values (areas). These values correspond approximately to the minimum and maximum values of these properties found during the numerous fits to the data, while maintaining an acceptable χ^2. That means that these errors include variations in the areas under the curves due to the use of different background functions, different neighboring lines, etc. The error of the percent exhaustion of the sum rule given later, however, is based on the standard deviation of the average sum rule exhaustion and is, therefore, more a measure for the fit to the models used than a measure for the total uncertainty. This is borne out by the observation that the standard deviation is always smaller or equal to the total uncertainty. In the table of final results we have given a total error based on the maximum and minimum value of the area under the curve found through the fitting procedure as described above, and on the error from the elastic cross section, which can be considerable, close to the minima in the elastic form factor.

C. Radiative corrections

Any scattered electron loses, with a certain probability, energy through emission of photons. It thus ends up in a lower energy bin than it would have in the absence of radiative processes, giving rise to the radiation tail. This subsection concerns itself with the loss in the integrated cross section due to these processes which occurs because the spectrum $d^2\sigma/d\Omega dE$ is integrated to an energy cutoff ΔE, and electrons with a loss greater ΔE will not be counted in the peak. This correction is different for photon emission which occurs in the field of the same nucleus as the scattering event itself (internal bremsstrahlung, giving rise to the Schwinger[22] correction δ_S), and photon emission which occurs in the field of another nucleus (external bremsstrahlung, giving rise to the bremsstrahlung[23] correction δ_B). The count rate for internal bremsstrahlung is proportional to the target thickness, the one for external bremsstrahlung is proportional to the square of the target thickness and puts, therefore, a limit on the target thickness which may be used.

The expression for the Schwinger correction is[22,24]

$$\delta_s = \frac{2\alpha}{\pi} \ln\left(\frac{E_i}{E}\right) (\ln q^2 - 1)$$

(q = momentum transfer) neglecting terms smaller than 0.01.

The bremsstrahlung correction is[15,25]

$$\delta_B = t \times \frac{4}{3}\left(1 + \frac{1}{9 \ln 184 Z^{-1/3}} \ln \frac{E_i}{\Delta E}\right)$$

(t = target thickness) neglecting terms smaller than ~0.01.

When applied to the measured and integrated elastic cross section both δ are exponentiated to account for multiple photon emission and thick target effects, respectively. The true integrated cross section then is related to the measured one by

$$\left.\frac{d\sigma}{d\Omega}\right|_{\text{true}} = \exp\left(\delta_S + \delta_B\right) \times \frac{d\sigma}{d\Omega}_{\text{exp}} .$$

With a cutoff energy of approximately 1 MeV [2 half-width (FWHM)] $e^{\delta_S} \approx 1.2$, and $e^{\delta_B} \approx 1.1-1.2$, depending on effective target thickness. Radiative corrections were applied only to the elastic area, because the area under an inelastic resonance is determined from resonance parameters by area $= \frac{1}{2}\pi\Gamma \times$ height and corresponds thus to integration to infinity, so that no cutoff energy is defined.[2]

It can be shown that it is justified to neglect the inelastic corrections for giant resonances if one follows Tsai's method[26] and divides the resonances in energy intervals with a width ΔE, e.g., equal to the width of the elastic line, and treats each interval as an isolated level with the excitation energy of the middle of the interval. One finds that the electrons which are scattered out of the interval through emission of photons are measured in intervals with lower electron energy (higher excitation energy).

Since the inelastic radiation tail falls off very fast and does, in contrast to the elastic one, not rise again,[27] the radiative corrections which were neglected influence the value of the integrated area measured very little (< 3%).

However, the above radiative effects result in an overall shift of the whole resonance to higher excitation energies. The influence on the relative strength of the same resonance in different spectra is even smaller than 3%, because the radiative corrections for the same resonance are nearly identical in different spectra, and do not influence, therefore, multipolarity assignments. Quite generally, it may be stated that radiative corrections in (e, e') do not pose a fundamental problem when the overall accuracy of the experiment is not better than 1 or 2%.[28]

D. Radiation tail

Three processes contribute to the radiation tail of the elastic peak, which is produced by the elastic electrons which have lost energy through these processes and are, therefore, measured at a lower electron energy E_f instead of E_i.

These processes are (1) radiation during scattering (internal bremsstrahlung) leading to the radiation tail proper; (2) radiation before or after scattering in the field of another nucleus (external bremsstrahlung); and (3) electron-electron (Møller) scattering. Landau straggling and ionization is important only close to the elastic peak and does not concern measurements of the continuum. The relative contribution of external bremsstrahlung and Møller scattering grow with target thickness t; they are called t^2 effects.

We feel that the difficulty in subtracting the radiation tail has been vastly overemphasized, as long as one aims at a final error of (10–15%) (excluding model dependence). This is borne out by the essential agreement between experiments in various laboratories which used quite different approaches, ranging from a free heuristic polynomial fit[29] to a very constrained background fit under inclusion of a calculated radiation tail.[16] In our experience it is more the fact that the resonances overlap which poses a problem. Nevertheless, the radiation tail of the elastic peak contributes somewhere between 50 and 90% to the total cross section, and any improvement would be helpful.

While reviewing the systematic body of data measured in Monterey between ^{28}Si and ^{238}U, we found evidence that it is *not* the radiation tail proper (internal bremsstrahlung) which poses a problem, but radiation before and after scattering, because the deviation between fitted total background after subtraction of constant room background and the calculated radiation tail using the formalism by Ginsberg and Pratt[30] was larger for thicker targets ($t > 1.0\%$ radiation length) than for targets with larger Z. This may, in part, be due to our energy range. It has been pointed out by Tsai[31] that some assumptions which enter the derivation of the formalism for the radiation tail (e.g., screening) do not work particularly well between 10 and 100 MeV.

For completeness, we give below the expressions for the effects which contribute to the radiation tail of the elastic peak.

The expression given by Ref. 30 for the charge radiation tail is

$$\frac{d^2\sigma}{d\Omega dE_f} = \frac{1}{m_0 c^2} \frac{Z^2 r_0^2}{4\pi\alpha} \frac{p_f}{p_i} \int_{x_{\min}}^{x_{\max}} \frac{dx}{x^2} F^2(x) R_{\text{ch}} ,$$

with $r_0 = 2.82$ fm (classical electron radius), p_i, p_f initial and final electron momentum, $x = \frac{1}{2}q^2$ (q, three momentum transfer), $F^2(\frac{1}{2}q^2)$ elastic form factor, and R_{ch} a lengthy kinematical expression.[30]

Since this expression has been derived in first order Born approximation (one photon exchange), it is not strictly valid for heavy nuclei, but the

influence of the nuclear electric potential (multiphoton exchange) can, somewhat heuristically, be taken into account by replacing $F^2(\frac{1}{2}q^2)$ by $F^2(\frac{1}{2}q^2, \theta)$ from experiments, in practice calculated with phase-shift codes from experimental values (only in PWBA is the cross section simply a function of q alone, if αZ is no longer small compared to unity, it becomes a function of two of the three variables E, θ, and q).[32]

Sometimes Schiff's peaking approximation is used, which leads to a simple analytical expression,

$$\frac{d^2\sigma}{d\Omega dE_f} = \frac{1}{m_0c^2}\frac{\alpha}{\pi}\frac{1}{E_i - E_f}\left[\left(1+\frac{E_f^2}{E_i^2}\right)\ln(2E_i\sin\theta/2) - \frac{1}{2}\right]\left(\frac{d\sigma}{d\Omega}(E_i) + \frac{d\sigma}{d\Omega}(E_f)\right).$$

However, for 90 MeV electrons the peaking approximation gives reasonable results only for $E_x \lesssim 10$ MeV.

The cross section for external bremsstrahlung

$$\frac{d^2\sigma}{d\Omega dE_f} = \frac{1}{m_0c^2}\frac{t}{2\chi_0}\frac{b}{E_i - E_f}\left(\frac{E_f}{E_i} + \frac{3}{4}\left(\frac{E_i - E_f}{E_i}\right)^2\right)\left(\frac{d\sigma}{d\Omega}(E_i) + \frac{d\sigma}{d\Omega}(E_f)\right),$$

$$b = \frac{4}{3}\left(1 + \frac{1}{9\ln 184 Z^{-1/3}}\right)$$

was taken from Mo and Tsai[26]; χ_0 is the radiation length.

Møller scattering finally is given by[23]

$$\frac{d^2\sigma}{d\Omega dE_f} = \frac{1}{m_0c^2}\frac{2\pi r_0^2 N t Z}{2 A}\left(\frac{1}{E_f^2} - \frac{2E_i - 1}{E_f(E_i - E_f)(E_i+1)^2} + \frac{1}{(E_i - E_f)^2} + \frac{1}{(E_i+1)^2}\right)\left(\frac{d\sigma}{d\Omega}(E_i) + \frac{d\sigma}{d\Omega}(E_f)\right)$$

with $2\pi r_0^2$ being the cross section of a classical electron and N Avogadro's number.

IV. RESULTS

A. General

In plane wave Born approximation (PWBA), valid only for $Z\alpha \ll 1$, the form factors are proportional to q^λ for low momentum transfer q (see, e.g., Ref. 33). While for $Z = 58$ PWBA evidently no longer is applicable, the q^λ dependence still is useful. Figure 4 shows the DWBA cross section divided by the Mott cross section (in light nuclei equivalent to the square of the form factor) as a function of momentum transfer. Since form factors are not a unique function of q in heavy nuclei, the curves are interpolations between cross sections taken from DWBA calculations with the correct primary ($\approx$ elastic) energy, E_i, used at the appropriate momentum transfer. This procedure is possible because, despite the breakdown of PWBA in general, we found that for constant primary energy E_i calculations of the form factors with different energy of the outgoing electrons E_f agree within 3% for the same q over an angular range from 30° to 175° (only 135° for the $E1$).

The broken vertical lines in Fig. 4 indicate the inelastic momentum transfer of the present data, for an excitation energy of 5 MeV. The method employed by us (interpolation of the calculated DWBA cross section as described above) has the advantage of not changing the measured values. Comparing the relative peak heights of Fig. 5 with the changes predicted by Fig. 4, some qualitative results are immediately evident. If we identify[2,3] the 12 MeV ($63A^{-1/3}$ MeV) and 25 MeV ($130A^{-1/3}$ MeV) resonance with $E2$, the states at 6, 22, and 31 MeV have a higher multipolarity. If we compare the energies in $A^{-1/3}$ units (31, 114, 160, respectively) with Table I, the first two are good candidates for an $E3$ assignment, while the latter lines up best with an $E4$ prediction. The resonance at 37 MeV is the most cumbersome to evaluate, because it is highest in energy and has the largest width. Comparison with Table I leads to an $E3$ assignment, but estimates based on sum rule considerations make $E0$ possible as well. The final assignments from DWBA calculations are indicated in Fig. 5, the ambiguities with the 31 and 37 MeV resonance will be discussed in detail later.

One also sees, that the ratio of $E1$ to $E2$ peak height (equal to the cross section ratio) does change very little, in agreement with Fig. 4, if taken at the correct q.

B. Giant dipole resonance and the nuclear breathing mode

More than 30 years ago Migdal[34] explained the nuclear photoeffect results of Bothe and Gentner[35] by assuming the existence of a dipole oscillation of the "protons against the rest of the nucleus" (the neutrons), an assumption leading to an average excitation energy for this mode of $24A^{-1/3}$

$(\beta Z/A)^{1/2}$ MeV, with β the coefficient of the symmetry term $\beta(N-Z)^2/A$ in the Bethe-Weizsäcker mass formula.[36] Several years later, independent developments led to the papers of Goldhaber and Teller[37] ($E_x \sim A^{-1/6}$) and Steinwedel and Jensen[38] ($E_x \sim A^{-1/3}$). Experimental evidence (see the review article by Berman and Fultz[39]) has shown, in the meantime, that neither model describes the energy of the dipole mode, the correct single A exponential law being $E_x \sim A^{-0.23}$.

The difficulty posed by the existence of two models for the GDR rests with the fact that they lead to quite different transition charge densities, which in turn, when used in DWBA calculations, produce form factors

$$F(q,E) = [(d\sigma/d\Omega)_{\mathrm{DWBA}}/(d\sigma/d\Omega)_{\mathrm{Mott}}]^{1/2},$$

which are different up to a factor of 2 in heavy nuclei.

The transition charge densities associated with Goldhaber-Teller (GT) and Steinwedel-Jensen (SJ) models are

$$\rho_{\mathrm{tr}}^{\mathrm{GT}}(r) = C^{\mathrm{GT}} r^{\lambda-1} d\rho_0(r)/dr$$

and

$$\rho_{\mathrm{tr}}^{\mathrm{SJ}} = C^{\mathrm{SJ}} j_1(r \times 2.08/c)\rho_0(r).$$

Photoabsorption measurements are practically model-independent: consequently, they cannot decide between different charge densities. While there have been many generalizations of the Goldhaber-Teller model (see, e.g., Ref. 40), only very recently a new detailed macroscopic approach to the problem has been tried by Myers, Swiatecki (MS) and co-workers,[41] who applied the framework of Myers's and Swiatecki's droplet model[42] to the problem of the giant dipole resonance. In short, their approach yielded a mixture of both modes,

$$\rho_{\mathrm{tr}}^{\mathrm{MS}}(r) = \frac{C^{\mathrm{MS}}}{1+\alpha}[\rho_{\mathrm{tr}}^{\mathrm{GT}}(r) + \alpha\rho_{\mathrm{tr}}^{\mathrm{SJ}}(r)],$$

with the constant α being a function of A, rising from approximately 0.5 for the Ni region to 0.8 for ^{208}Pb. Myers *et al.*[41] give three solutions to their model, the supersimple solution, the droplet mode, and the exact solution (nomenclature of Ref. 41), with the parameter α being 0.80, 0.74, and 0.64, respectively, for $A = 140$.

Aside from the fundamental importance of the correct description of the giant dipole resonance, this knowledge is needed for a different reason. There has been mounting evidence recently of the existence of a giant monopole resonance at $80A^{-1/3}$ MeV in heavy nuclei, exactly under the GDR. This excitation energy was originally proposed by Marty *et al.*,[43] the strongest support coming from (α, α)

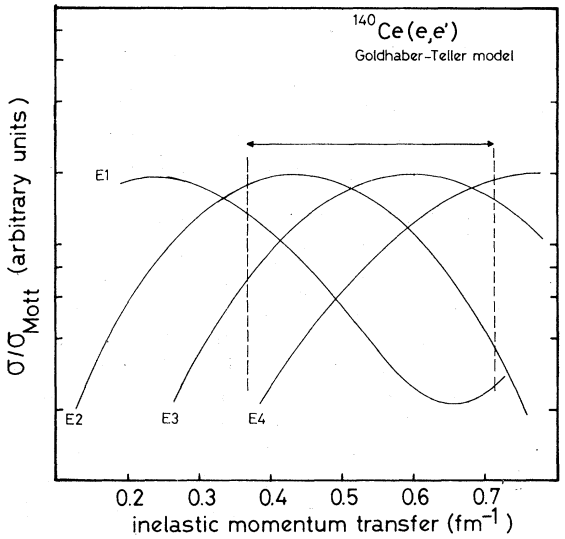

FIG. 4. Comparison of DWBA cross sections for $E1$ to $E4$ transitions divided by the Mott cross sections. The curves are interpolations between calculations for the correct energy and angle of the five measurements used, since the data in this work and from Ref. 2 vary greatly in electron beam energy. The curves were normalized so that the first maxima are equal. The program of Tuan *et al.* (Ref. 52) was used with a transition charge density $\rho_{\mathrm{tr}}(r) = Cr^{\lambda-1}d\rho_0(r)/dr$.

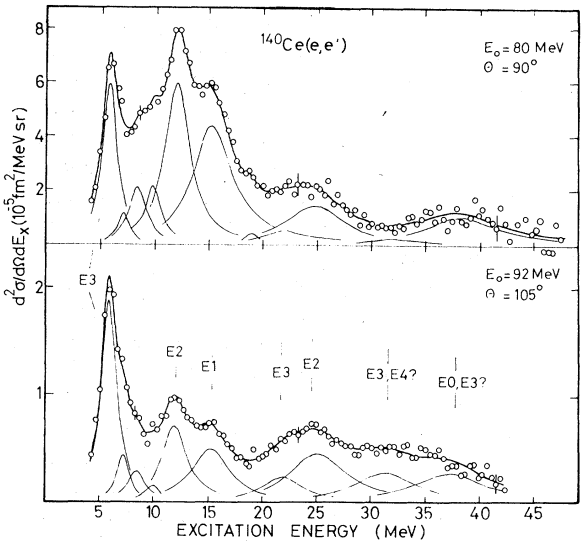

FIG. 5. Data of Fig. 2. after the fitted background (consisting of the radiation tail, the general room background, and experimental background) and the "ghost peak" as described in the text have beem subtracted. These two spectra are shown together so that the shrinkage of smaller multipolarity transitions versus the growth of higher multipolarity transitions may be seen. The relative change in peak heights of the single resonances indicate very clearly the various multipoles contributing. Note, e.g., that the $E2$ cross sections fall off more than a factor of 6 between the 80 MeV and the 92 MeV spectra.

scattering at very forward angles.[44] This evidence is very convincing, but not conclusive, because it is based on the assumption that (α, α') does not excite the isovector GDR resonance, the α particle being a $T=0$ particle. However, the α particle does have a charge and, therefore, breaks isospin selection rules, and, probably more importantly, the nuclei where this mode has been investigated by (α,α), ^{208}Pb and ^{144}Sm, have a large neutron excess, giving rise to isospin impurities in α scattering of the order $(N-Z)/A$. In addition, isospin impurities in the GDR have even been found with capture reactions in light self-conjugate[45,46,47] nuclei and in nuclei with small neutron excess[46,48] up to $A=52$. Unfortunately, in heavier nuclei capture reactions cannot be used to investigate the GDR, because of the rising Coulomb threshold and the falling energy of the dipole resonance. Little is known, therefore, about isospin impurities in these nuclei.

Electron scattering is very suited to exciting a monopole oscillation, but is hampered in general by the well-known property of an $E0$ excitation to exhibit the same momentum transfer (or angular) dependence as the $E2$, and in particular, that is for a monopole mode at $80A^{-1/3}$ MeV, by the presence of the GDR. Any (e, e') experiment which attempts to investigate the problem of the monopole, has first to solve the problem of the model for the GDR, because the latter has to be subtracted in order to get the monopole cross section, and the choice of the model determines the result. In our opinion this problem is mainly a question of good enough statistical and systematic accuracy over a wide enough range of momentum transfer in order to pin down the experimental form factor. Past (e, e') experiments, including our own, have not achieved this goal.

Despite these uncertainties, the existence of a monopole resonance at $80A^{-1/3}$ MeV has been supported by (e, e') measurements at high primary energy and forward angles, using multipole expansion,[49] the result being that 100% of the monopole sum rule is exhausted if one uses the GT model for the GDR but finding only 10% when using the SJ model. It might be noted, that these results are in contrast to earlier evaluation of the same data using a line shape fit by the same authors. Similar results[50] have been given for ^{208}Pb.

Since the multipole expansion introduces a nuclear model *before* the cross sections are extracted, it is not possible to make a decision between the models with this method. The low primary energy electron scattering experiments[2,51] ($E_0 \lesssim 70$ MeV), on the other hand, are unsuited to explore this problem, because in order to reach the necessary momentum transfer, backward angle ($\theta \gtrsim 120°$) scattering has to be used. Two problems enter here. The DWBA code[52] with retardation (excitation energy >0) fails for the $E1$ at backward angles[2] (that it converges at all at more forward angles is due to accidental cancellation of two terms[53]). As can be clearly seen in the form factor,[3,29,51] an unphysical upswing occurs at backward angles. A way around this is to neglect retardation (excitation energy $=0$) and to take the form factor at the correct inelastic momentum transfer

$$q_{\mathrm{in}} = (E_i^2 + E_f^2 - 2E_i E_f \cos\theta)^{1/2}/\hbar c$$

instead.[54,55]

In addition, to add one more layer of ambiguity, there are transverse contributions to the cross section in the GDR regions. This is evident when one uses DWBA calculations without retardation as described before, because a large cross section remains at backward angles in excess of that expected from forward angle (e, e') measurements at the same momentum transfer, and from (γ, n). Assumption of a transverse electric spin flip $E1$ is compatible with the data,[2,3,4] but the experimental evidence is not conclusive. Furthermore, there might be an $M2$ (Ref. 2) or $M3$ (Ref. 21) resonance in the GDR region. Since both effects (failure of DWBA at large angles, transverse contributions) go in the same direction, the problem has apparently not been recognized in recent low energy electron scattering experiments.[21,51]

In order to convince ourselves that there is a real problem with the DWBA formalism in its present form,[53,55] and not a problem of suitable choice of integration parameters, we have done extensive $E1$ calculations with the program of Tuan *et al.*, which to our knowledge is the basis for most calculations performed in various laboratories.[56,57] The standard test for (e, e') DWBA is to compare the DWBA results for $Z=0$ with PWBA, because the latter can be solved in closed form. Both should be identical. The subroutine which selects the integration parameters depending on primary energy, number of partial waves, etc., gave for 65 MeV agreement only up to approximately 140°. Since series of spherical harmonics have poles at the origin, we used the reduction method of Ravenhall *et al.*[58] to improve upon the convergence. The program, which has one reduction built in, was changed to allow for multiple reductions. Using more reductions made the convergence at forward angles worse, which is understandable because more poles are removed at the origin than exist,[55] but it improved the backward convergence for $Z=0$ dramatically. With four reductions DWBA ($Z=0$) and PWBA agreed to better than $\frac{1}{2}$% up to 180°, but only when the radial

integration was extended to greater than 500 fm, instead of 50 to 100 fm which are sufficient for higher multipolarities. However, this work turned out to be nearly for naught because DWBA ($Z \neq 0$) still diverged at backward angles, $\theta > 150°$, the divergence becoming more pronounced with lower primary energy, that is, with a rising E_x/E_i ratio.

In the attempt to solve the problem of the $E1$ form factor, we have only used measurements with $90° \leq \theta \leq 105°$, thus avoiding the whole complex of transverse contributions. DWBA calculations show (Fig. 6) that in order to be able to differentiate between the GT, SJ, and MS models for ^{140}Ce, an accuracy of 25% or better for the single measurement is necessary. To differentiate between the various solutions of Myers *et al.*, one needs an accuracy of better than 10%. While the latter is difficult to achieve in general, it is possible for the $E1$ in the case of ^{140}Ce. For once, the line shape of the GDR is known from (γ, n),[59] and, secondly, the already described separation of the $E1$ and $E2$ resonances in $N = 82$ nuclei is important. The essential element, however, is the fit over a very wide range of excitation energy, which puts a strong constraint on the freedom in the background fitting. In addition, our finding that radiation tail calculations are good up to 20–25 MeV agrees with Szalata *et al.*,[60] who used comparable primary energies for ^{20}Ne. Sasao and Torizuka[50] even claim 80 MeV as limit for ^{208}Pb, which might be possible, because of their much higher primary energy (see remark in Sec. III D). Since the GDR in ^{140}Ce is well below 20 MeV, the cross section turned out to be very background insensitive, much more so than the resonances below 10 MeV, where the accuracy in our installation is hampered by the ghost peak, and the ones above 20 MeV, due to their large width.

We have used a fitting procedure described recently[17] to fit the (γ, n) data[59] for ^{140}Ce, resulting in $E_\gamma = 14.95 \pm 0.05$, $\Gamma = 4.20 \pm 0.05$, and $\sigma = 384$ mb. The difference in cross section to the values given by Berman[61] is mainly due to the inclusion of the isovector GQR at 25 MeV. The difference in excitation energy is due to the fact that we have fitted the $E1$ strength function rather than the (γ, n) cross section.[17] Our result for the (γ, n) cross section corresponds to a $B(E2, q = k) = 41$ fm^2 or $B(E\lambda, q = 0) = 43$ fm^2, the latter quantity to be used in electron scattering.

Nevertheless, we have fitted the GDR parameters in the (e, e') spectra, despite the knowledge about the line shape (E_x, Γ) from (γ, n). The results are $E_x = 15.3 \pm 0.1$ and $\Gamma = 4.4 \pm 0.2$. The excitation energy is higher than the (γ, n) energy outside the error. A similar shift has been reported earlier for $N = 82$ nuclei.[2,62] Because of our unified approach of fitting the strength distribution rather than the cross section in (e, e') and (γ, n) data, the explanation given in Ref. 2 for an even larger shift now no longer applies for the shift found.

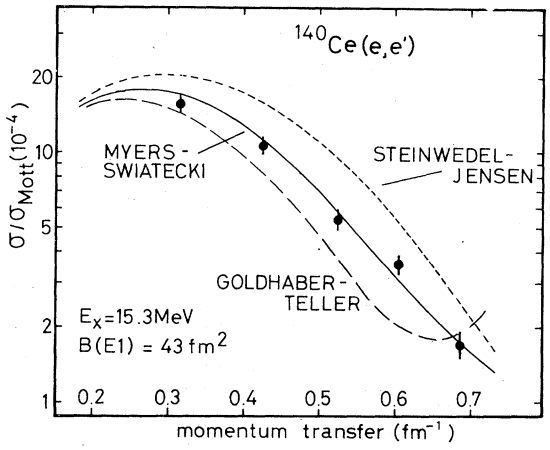

FIG. 6. Comparison of the DWBA and experimental form factors for the resonance found at 15.3 MeV. The experimental form factors are compared to the Goldhaber-Teller, Steinwedel-Jensen, and Myers-Swiatecki models. The mixed model of Myers, Swiatecki *et al.* (Ref. 41), explained in the text, fits the experimental data best. A mixture ratio of GT mode to SJ mode of 0.76 ± 0.04 was found, corresponding to the droplet mode of Ref. 4. The curves are not fitted to the (e, e') data, but to the photon measurement of Ref. 59.

We believe that the remaining difference in excitation energy is due to the shift produced by the radiation tail, described in Sec. III C, but this assumption could only be proven by applying Tsai's unfolding procedure,[26] which we have not done, because this would add one more layer of data manipulation without improving the accuracy in cross section determination.

Figure 6 shows the final result for the resonant cross section found at 15.3 MeV. We must emphasize that the curves shown (GT, SJ, MS) are *not* fitted to the data. They were normalized to $B(E\lambda, q = 0) = 43$ fm^2 from the (γ, n) data.[59] There is a small inconsistency in our procedure insofar as we have measured on a $^{\text{nat}}$Ce target, while the (γ, n) data were taken on enriched isotopes, but the ^{142}Ce resonance values[59,61] are so close to ^{140}Ce, that the change is negligible for our purposes.

In order to investigate the three solutions of the MS model, we have fitted the model parameter α to our data, while keeping the B value to 43 fm^2, resulting in $\alpha = 0.74 \pm 0.04$, thus corresponding to the droplet mode.[41] While at first glance our result seems to rule out a monopole under the giant dipole resonance, more discussion is needed.

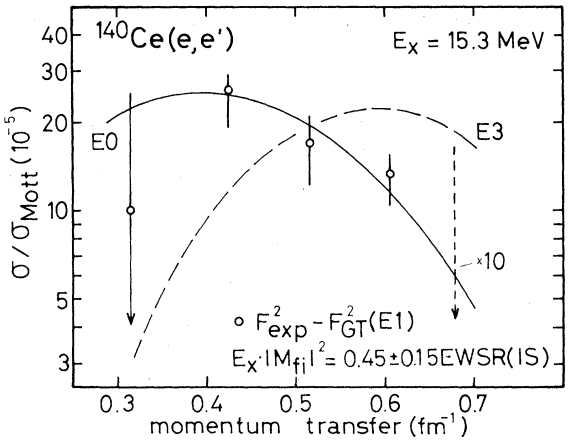

FIG. 7. Comparison of the difference between the experimental form factors and the Goldhaber-Teller model (see Fig. 6) to the DWBA form factors for the resonance found at 15.3 MeV. The difference shows that the possibility of an $E0$ transition with $(45 \pm 15)\%$ of the monopole isoscalar sum rule lying beneath the dipole exists only if the Goldhaber-Teller model is assumed to be correct.

Figure 6 clearly rules out the SJ model, however, because it is higher than the experimental points by nearly a factor of two. But because the GT form factor is lower than the data, the difference between the GT and MS models could be due to a resonance of different multipolarity. Figure 7 shows, therefore, the difference between the experimental points and the GT curve of Fig. 6. The difference is nicely described by an $E2$ or $E0$ form factor. If one chooses the latter, $(45 \pm 15)\%$ of the energy-weighted sum rule (EWSR) ($E0, \Delta T = 1$) would be exhausted, in near agreement with,[44] which gives $(100 \pm 20)\%$, but reports a model dependence of a factor of two. For the monopole calculations the model by Schucan[63]

$$\rho_{\mathrm{tr}}^{E0}(r) = -3\rho_0(r) + d\rho_0(r)/dr$$

was used, which is identical with one of two used by Satchler[64] and Youngblood *et al.*,[44] except for the difference between charge and nuclear matter oscillation in (e, e') and (α, α'), respectively. The DWBA code used by us is a version of that of Tuan *et al.*[52] written by Kawazoe.[57] We have also tried the second model of Satchler[64]; differences between the two are below 10% in the momentum transfer region covered by our experiment.

Table II shows the parameters for monopole resonances reported in $N = 82$ nuclei. In contrast to the $E1$ results, shown for ^{140}Ce and ^{142}Nd in Table III, there is a wide variation in strength and excitation energy. Especially for the excitation energy, not model dependent like the strength, the difference is difficult to explain for a giant resonance, which is expected to change slowly with A.

There are two arguments against the interpretation that the difference between experiment and the GT model shown in Fig. 7 is due to a monopole or quadrupole excitation.

1. Since the claimed monopole has a width of 2.5–3.0 MeV in heavy nuclei,[43,44,65] it can be seen from the difference between experiment and GT curve, compared to the value of the GT curve itself in Fig. 6, that it would have a peak height greater than the $E1$ at $q = 0.52$ and $q = 0.61$ fm^{-1}. The apparent width of the composite line $(E1 + E0)$ then should be noticeably smaller in our fits than the width known from (γ, n). If we make the conservative estimate that the peak heights are equal, $\Gamma(E0 + E1) = 3.5$–3.7 MeV compared to $\Gamma_{\mathrm{fit}} = 4.4 \pm 0.2$ MeV. However, because of the problems encountered with the choice of background in hadron scattering, we would not put very much emphasis on this argument.

2. More convincing, therefore, is the independent confirmation of the MS model through the single power A law for the GDR. The MS model reproduces $E_x \sim A^{-0.23}$ MeV known from experiment and consequently rules out the GT model unambiguously. Use of the MS model instead of the GT model in other (e, e') experiments which find monopole strength at $80\ A^{-1/3}$ MeV will eliminate most or all of the $E0$ strength within the errors given.

As outlined earlier in this subsection, isospin is not necessarily conserved in α (and d) scattering from $(N - Z) > 0$ nuclei, and rather large isospin impurities have been found in the GDR in such nuclei accessible to capture reactions, which mostly do not have a large neutron excess. For example, comparing the (e, e') ^{40}Ce data of Goldmann[66] and the ^{36}Ar$(\alpha, \gamma_0)^{40}$Ca data of Watson *et al.*[47] with the $E0$ data of Marty *et al.*,[43] a very close agreement of width and position of the $E1$ GR with the proposed monopole is found ($E_x = 20$ MeV, $\Gamma = 4$ MeV). If we would apply the background procedure of hadronic scattering, and of Ref. 66 (matching of a linear background to the data at the energy where the spectra start to be flat) to our data, an apparent width of the 15.3 MeV resonance of 2.5–3.0 MeV would result. The position of the monopole claimed in ^{40}Ca gives even more reason to believe that the $E1$, and not the monopole, is seen in $(\alpha, \alpha')^{44}$ and $(d, d')^{43}$ scattering, because its excitation energy ($68\ A^{-1/3}$ MeV) scales exactly with the GDR, down from $81\ A^{-1/3}$ MeV in ^{208}Pb. From the very constant $A^{-1/3}$ dependence (Fig. 1) of the isoscalar $E2$, one would not expect such a strong variation for the isoscalar breathing mode.

On the other hand, the excitation mechanism for $E0$ and $E1$ excitation is well understood for

TABLE II. $E0$ strength at $80\,A^{-1/3}$ MeV in $N = 82$ nuclei.

Nucleus	Reaction Method	E_X (MeV)	Γ (MeV)	R [a]	Ref.
^{140}Ce	(e,e')			45 ± 15 [b]	this work
^{142}Nd	(e,e')	16.2 ± 0.2	3.00 ± 0.15	28 ± 10 [c]	21
^{144}Sm	(e,e')	14.8 ± 0.2	2.40 ± 0.15	20 ± 10 [c]	21
^{144}Sm	(α,α')	15.1 ± 0.5	2.9 ± 0.5	100 ± 20 [c]	44

[a] $R = E_X |M_f|^2 / \mathrm{EWSR}(E0, \Delta T = 0) \times 100$.
[b] Strength based on difference between experiment and the GT form factor.
[c] Line shape fit.

(e,e'), and 100% EWSR $(E0, \Delta T = 0)$, as proposed, would be visible. We think, therefore, that more work is needed on the understanding of the excitation mechanism of $T = 0$ hadronic particles beyond the argument that they just do not excite the $\Delta T = 1$ GDR.

Since we did not measure backward angles, we cannot experimentally contribute to the solution of the question, whether the "excess" strength of the GDR at backward angles is due to electric $E1$ spin-flip[67] or $M2$ or $M3$ contributions.[2,51] However, we can rule out that they are due to longitudinal excitations.

C. Quadrupole excitations and the total photon cross section

The giant isoscalar quadrupole resonance in nuclei (GQR, $\Delta T = 0$) is probably the best investigated of the "new" (how long have they been there?) resonances. It corresponds to a jump between single particle orbits which have quantum numbers different by 2. In contrast to the case of the GDR, the hydrodynamic models completely fail to predict this mode of excitation. The flood of information produced in recent years, following the first discovery of the $E2$ $(\Delta T = 0)$ mode,[7] have, in contrast, shown that the ideas of Bohr and Mottelson concerning the interplay between single particle and collective coherent motion in the nucleus and especially including the role of isospin, were correct.[11] The scattering of strongly interacting particles, especially α's[13] have played an essential role in the systematic investigation of the isoscalar giant quadrupole resonance, but the potential structural richness of the giant resonance region has, up to now, mainly been fully open to electro-excitation, because isovector excitations are suppressed in hadron scattering.[18] Capture reactions, while one of the most versatile tools in light nuclei,[1,68] are hampered by the rising Coulomb threshold in heavy ones.

In general, good agreement has been found for the sum rule strength extracted from (α,α') and (e,e'), e.g., $(92 \pm 25)\%$ (Ref. 13) vs $(92 \pm 10)\%$ (Ref. 69) in the case of ^{208}Pb, or $(54 \pm 15)\%$ (Ref. 13) vs $(56 \pm 6)\%$ (Ref. 16) the case of ^{90}Zr and ^{89}Y. There has been some controversy concerning position and width in $N = 82$ nuclei,[13,70] but this discrepancy has been resolved with α scattering of higher energy, which showed a satellite at $80A^{-1/3}$ MeV,[44] interpreted as $E0$ (see discussion in the previous subsection, but also Ref. 71). A closer look into $N = 82$ nuclei shows some inconsistencies, which occur very systematically, although they are not in all cases outside the range of overlapping er-

TABLE III. $E1$ strength in $N = 82$ nuclei.

Nucleus	Method	E_X (MeV)	R [a]	Model	Ref.
^{140}Ce	(γ,n)	14.95 [b]	124	MI [c]	61
^{140}Ce	(e,e')	(15.1) [d]	121	GT	2
^{140}Ce	(e,e')	15.3 [b]	124 [e]	MS [e]	this work
^{142}Nd	(γ,n)	14.90 [b]	130	MI [c]	61
^{142}Nd	(e,e')	15.4 [f]	129	GT	62

[a] $R = E_X B(E1,0)/\mathrm{EWSR}(E1, \Delta T = 1) \times 100$.
[b] Peak of the strength distribution.
[c] Practically model independent.
[d] Was taken from (γ,n).
[e] With $\alpha = 0.74$.
[f] Peak of the cross section.

rors. To find these discrepancies one has to look into the method of evaluation. The (e,e') spectra have mostly been evaluated with a line shape fit using either Lorentz lines for the cross section (e.g., Refs. 2, 62, 72), or Breit-Wigner curves for the B-value distribution (strength function),[16] and it has been shown that the two approaches are nearly equivalent to each other, at least they do not change the resulting areas under the strong resonances noticeably.[17] In contrast, (α,α') data could not be described as well by a Lorentz curve as by a Gaussian.[13] Positions and width from a direct evaluation of the data (rms-energy, rms-width) agreed within 100–200 keV with width and centroid position from Gauss or Lorentz fits, but the Lorentz fits resulted in 20–30% increase in peak yield, because more strength is under the tails, which do not fall off as rapidly as for the Gaussian.[13]

Since the areas under a Lorentz and a Gauss curve of equal width and height are different by a factor of $\ln 2$,[17] the (e,e') results should be 44% larger, everything else equal (that the effective yield going from Gauss to Lorentz curves changes only 20–30% as reported in Ref. 13 and not by 44%, is understandable, because line shape fits have a tendency to conserve the area). In fact, as Table IV shows, just the opposite occurs, namely the (α,α') data are systematically higher, even the introduction of the $80A^{-1/3}$ MeV resonance in the analysis reduces the sum rule strength only from 91% to 85% (Ref. 13 vs 44 for ^{144}Sm in Table IV). The last value in Table IV, from the current measurement, under inclusion of the 93° spectra of Ref. 2 is markedly lower than the result of old analysis for ^{140}Ce or any of the other low energy (e,e') results,[29,62,70] although it agrees within the errors with the others (except ^{142}Nd (Refs. 29, 70) which is marginally outside the errors). Figure 8 shows why. The lower energy measurements span too small a momentum transfer region at forward angles to be able to recognize the systematic behavior of the cross sections, namely a deviation from the Goldhaber-Teller (GT) model. If one, not considering the standard deviation of the experimental points from the curve, does a fit of the "strict" ($c_{tr}/c = 1.0$, nomenclature of Ref. 73) GT model to the data, a strength of 65% EWSR results. But obviously, the data do not fall on this curve. The solution to this discrepancy is ambiguous. Either the model fails, or another (or several) underlying higher multipolarities (Fig. 4) contribute. Figure 8 shows the solution to the first possibility, namely a fit of the model parameter c_{tr}/c to the data, which reduces the B value from 2500 fm^4 to 2000 fm^4. Since it has been shown, both with microscopic calculation[74] and with more fundamental consideration[11,75] that an $E2$ state which carries a major fraction of the sum rule should follow the hydrodynamical model closely, we prefer the alternative explanation. Figure 9 thus shows the difference between the experimental points and the GT model of Fig. 8, clearly favoring an $E3$ assignment for the assumed underlying cross section. Despite this ambiguity in interpretation, the $B(E2)$ would be reduced in either case to approximately 2000 fm^2. But an $E4$ cannot be ruled out, especially if one realizes that the result is doubly model dependent, insofar as the "experimental points", too, depend on the DWBA calculations used in Fig. 8.

Table V shows the $E2$ strength up to 12 MeV from (e,e'); a total of 67 to 77% of the EWSR is exhausted depending on whether or not the 10 MeV state[2] is counted. Since the latter coincides with the $53A^{-1/3}$ state in ^{208}Pb,[4] which may or may not be part of the monopole GR,[69,76] we will come back to that point in a separate section later.

There is a corresponding number of microscopic calculations to the experimental attention the isoscalar $E2$ (and isovector) mode has had in recent years. Historically the first such calculation has been published by Kamerdzhiev[77,78] followed by Ring and Speth[79] and Bertsch.[80] We would like to point out that Ref. 77, being submitted at the same time as Ref. 3, is the only microscopic calculation which truly predicted very accurately both isoscalar and isovector $E2$ in ^{208}Pb and ^{120}Sn. The most detailed results have been published by Liu and Brown.[81] Though they do not treat ^{140}Ce explicitly, their results show a regularity concerning A dependence, and we have interpolated their ^{90}Zr and ^{208}Pb calculations (Table VI) to compare with our data. Although it would be easily possible with our DWBA code to use the microscopic transition densities from one author or the other, we have abstained from doing so, not only for the reason already given above, but also to preserve compatibility between different laboratories. (Transition densities from macroscopic models are easily available and comparable, microscopic ones are not.) The (α,α') data show convincingly, that the Goldhaber-Teller model describes the isoscalar $E2$ and $E3$ data over many maxima and minima, even though there is an inherent difficulty to extract the electromagnetic strength unambiguously from strong interacting particle scattering.[82]

In contrast to the isoscalar $E2$, it is not expected from the isovector mode to simply follow a surface oscillation.[11] The Goldhaber-Teller and Steinwedel-Jensen model has been applied separately to the isovector mode in ^{208}Pb by Sasao and Torizuka within their multipole expansion.

TABLE IV. Comparison between (α,α') and (e,e') experiment for the 12 MeV resonance in different $N = 82$ nuclei show the α results to be systematically higher. A detailed look at the different evaluation procedures and line shapes used, as discussed in the text, shows that the (α,α') results should be 20 to 30% lower than the (e,e') data, because this would be the effective difference of the yield of a Lorentz or Breit–Wigner fit vs a Gaussian line shape. Effectively, the (e,e') sum rule values are 20 to 30% lower, making the difference even more markedly. The new (e,e') ^{140}Ce value, (50 ± 10)% EWSR, is lower than the older ^{140}Ce and ^{142}Nd data because a wider range of momentum transfer was covered, Figures 8 and 9 show that there is an ambiguity in the interpretation as to whether the difference to the strict Goldhaber–Teller model ($\rho_{tr} \sim d\rho_0/dr$) is due to other multipolarities ($E3$ and $E4$), or to a failure of the model. However, the low value of the sum rule results independent of this ambiguity. The newest (α,α') position and width for ^{144}Sm (Ref. 44) is now in essential agreement with the electron data.

Nucleus	E_X (MeV)	Γ (MeV)	R [a]	Model	Method	Ref.
^{140}Ce	12.0 ± 0.2	2.8 ± 0.2	66 ± 20	GT	(e,e')	2
^{142}Nd	12.0 ± 0.2	2.8 ± 0.2	65 ± 13	GT	(e,e')	62
^{142}Nd [b]	13.2 ± 0.4	3.6 ± 0.3	110 ± 30	GT	(α,α')	13
^{142}Nd	12.0 ± 0.2	2.9 ± 0.3	73 ± 9	GT	(e,e')	29, 70
^{144}Sm	11.9 ± 0.2	2.9 ± 0.2	[c]	GT	(e,e')	70
^{144}Sm [b]	13.0 ± 0.3	3.9 ± 0.2	91 ± 25	GT	(α,α')	13
^{144}Sm	12.4 ± 0.4	2.6 ± 0.4	85 ± 15	GT	(α,α')	44
^{140}Ce	12.0 ± 0.2	2.9 ± 0.2	51 ± 10 [d]	GT [e]	(e,e')	this work

[a] $R = E_X B\,(E2, q = 0)/\text{EWSR}\ (\Delta T = 0) \times 100$.
[b] Energy, width, and strength not corrected for assumed monopole at 15 MeV.
[c] Strength not given.
[d] Total error. Standard deviation results in (51 ± 5)% EWSR.
[e] $c_{tr}/c = 0.95$, see text.

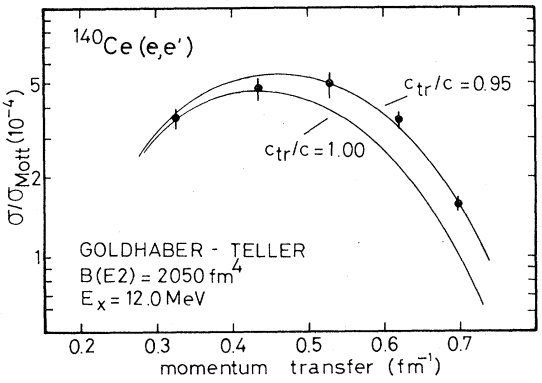

FIG. 8. Comparison of the DWBA and experimental form factors for the resonance found at 12 MeV. The Goldhaber-Teller model for an $E2$ transition was fit to the experimental data (Table X) first using as the half-density radius $c_{tr} = c$, and secondly $c_{tr} = 0.95c$ as explained in the text.

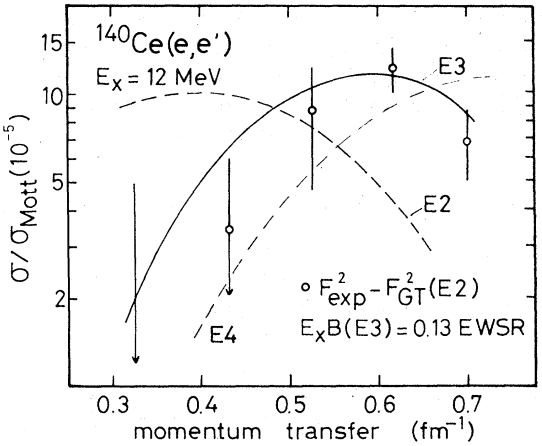

FIG. 9. Comparison of the difference between the experimental form factor and the Goldhaber-Teller model $E2$ DWBA form factor with $c_{tr} = c$ (see Fig. 8) to $E3$ and $E4$ calculations for the resonance found at 12 MeV. The difference shows that an $E3$ transition beneath the $E2$ transition found at 12 MeV may exist if the Goldhaber-Teller model is assumed to be correct. A sizable $E4$ contribution may not be ruled out.

TABLE V. Strength of all identified $E2$ states up to 12 MeV as determined by (e,e') (Ref. 2). They sum up to 77% of the isoscalar sum rule if one includes the 10 MeV state, and to 67% without. The assignment for the 10 MeV state is ambiguous for two reasons. First, (e,e') cannot easily distinguish between $E0$ and $E2$, and secondly, this state has not been seen in hadron scattering, possibly indicating either monopole or isovector character. Thus, this resonance might be (1) a second branch of the isoscalar GR at 12 MeV, (2) part of the monopole resonance with 13% of the EWSR ($E0$, $\Delta T = 0$) or, (3) due to an oscillation of the excess neutrons (Ref. 11). While a force which produces a separate excess neutron osscillation is difficult to imagine (Ref. 98), the same is true for case (1). Against the monopole interpretation speaks mainly the low sum rule value, leaving the nature of this state as unsolved question, with the excess neutron oscillation slightly favored, because it is the only explanation which consistently explains the data.

E_X (MeV)	B (fm^4)	Γ_γ^0 (eV)(10^{-3})	R [a]	Ref.
1.60	2.71×10^3	4.6	9.2	2
2.90	2.87×10^2	9.5	1.6	2
3.12	5.44×10^2	26	3.6	2
3.32	2.92×10^2	19	2.0	2
10.0 [b]	4.30×10^2	7590	9.1	this work
12.0	2.01×10^3	80700	51	this work

[a] $R = E_X B\,(E2,0)/\mathrm{EWSR}(E2, \Delta T = 0)\times 100$.
[b] Interpretation ambiguous.

The same argument as for the dipole mode is valid; since the multipole expansion introduces a model already for the extraction of the cross sections, a model dependence cannot be investigated. Our line shape fit shows a resonance at 25 ± 1 MeV with a width of 6.6 ± 1 MeV (FWHM). As in the case of the isoscalar resonance, we find a deviation between cross sections and DWBA GT calculations. Figure 10 shows, among transitions to other resonances, which will be discussed later, that the strict GT model does not describe the 25 MeV data, but also that an $E3$ form factor does even worse. Although there has not yet been a quantitative extension of the work by Myers *et al.* for description of the $E2$ mode, we have fitted a parameter $\alpha(E2)$ in analogy to the $E1$ resonance[41]

$$\rho_{\mathrm{tr}}^{\mathrm{MS}}(r) = \frac{C^{\mathrm{MS}}}{1+\alpha}\left[\rho_{\mathrm{tr}}^{\mathrm{GT}}(r) + \alpha(E2)\rho_{\mathrm{tr}}^{\mathrm{SJ}}(r)\right],$$

with $\alpha(E2) = 1.0\pm0.6$ determined experimentally. Figure 10 shows that the "Myers-Swiatecki" model reduces the standard deviation compared to the GT model.

Figure 11 shows the alternative interpretation: analogous to Fig. 9 the difference between experimental points and the GT model is plotted as a function of momentum transfer and compared to DWBA form factors. Either $E3$ (~20% EWSR) or $E4$ (~60% EWSR) strength, or both, may be hidden under the 25 MeV resonance. Table VI shows that both multipolarities would be compatible with the microscopic calculations.[81] As in the case of the isoscalar $E2$ both interpretations result in a lower $B(E2)$ value, 50% EWSR ($\Delta T = 1$), compared to 80% for the strict GT model. It is clear from the foregoing that in this case we favor the MS model interpretation over the interpretation of underlying other multipolarities, but clearly a more thorough investigation in terms of the droplet model, as done in Ref. 41 for the $E1$, is needed.

This leaves us with the overall result that only approximately 50% of isoscalar and isovector strength are concentrated in form of a coherent resonant state of 12 and 25 MeV, respectively. The question of where the missing $E2$ strength might be is of great importance. It could be either dispersed into a nonresonant background, or it could be pushed up to higher excitation energies through short range correlations[5,11] as already mentioned. If we assume the latter, an interesting possibility opens up. Intrigued by the total γ-absorption measurement of the Mainz group[83] and the small percentage of $E2$ strength found in a concurrent measurement on ^{28}Si (Ref. 84), we have calculated for ^{28}Si the amount of photon cross section which could be due to $E2$ absorption at high excitation energy.

The total photon absorption measurements[83] found that two times the classical $E1$ sum rule $60NZ/A$ MeV mb (Thomas-Reiche-Kuhn[85]) were exhausted up to the pion threshold. No disentangling into different multipolarities has yet been possible (see, e.g., editors comments in Ref. 86, Part VI). While our measurement[84] in ^{28}Si does not disentangle multipolarities above 50 MeV either, it is nevertheless illuminating to calculate how much of the $E2$ strength missing below 50

TABLE VI. Comparison between (e,e') results (Ref. 2 and this work) and the calculations of Liu and Brown (Ref. 81). We want to emphasize that the calculations were not performed directly for ^{140}Ce, but are interpolations between ^{90}Zr and ^{208}Pb. We have left out the $E1$ calculations, because as in other cases, they "were singularly unsuccessful in obtaining the position of the giant dipole resonance", [G.E. Brown, Asilomar Conference 1973, $p.$ 57]. For the other multipolarities, one might state that the present calculations do rather well describe not only the position, but also the strength distribution, particularly in the case of the $E3$ strength, which generally has been found to be much more distributed than the $E2$. In some cases ambiguities result in the assignment of the experimental strength, denoted by footnotes. In any case the text and tables should be consulted before fast conclusions are drawn.

		Theory (Ref. 81)		Experiment	
λ	T	R [a]	E_X(MeV)	R [a]	E_X(MeV)
0	0	34	19	45	15
		55	21–27		
	1	9	11–21	(13) [b]	10
		80	21–50	130 [c]	37
2	0	15	6	16	1.5–3.4
		65	12	50	12
		10	17–27		
	1	13	0 –23	(9) [b]	10
		65	23–32	50	25
		20	32–50		
3	0	18	6	19	6
		7	10	(5)	7.4
		12	12–18	(8) [d]	12
		39	18–28	19, (20) [d]	22, (25)
		13	28–37		
	1	14	13–28		
		65	28–43	75 [c]	37
		15	43–60		
4	0	26	0 –18	4 + (7) + (20) [d]	2.1, 7.4, 12
		40	18–40	(60) [d]	25
	1	17	0 –30		
		70	30–70	80	31

[a] $R = E_X B\,(E\lambda,\ q=0)/\mathrm{EWSR}(E\lambda, \Delta T)\times 100$.
[b] Ambiguous, see caption to Table V.
[c] Data compatible with both $E0$ and $E3$.
[d] Difference to GT $E2$ form factor, compatible with both $E3$ and $E4$.

MeV would contribute if it is located higher in excitation energy. It was found that nearly all the γ cross section in excess of the Gell-Mann-Goldberger-Thirring sum rule[87] (GGT = 1.4 times the classical $E1$ sum rule) under certain conditions might be due to $E2$ absorption.

Since the γ cross section and the reduced transition probability $B(E2,k)$ are connected by[17]

$$\sigma_\gamma dE_\gamma = 3.1\times 10^{-6} E_x^{\,3} B(E\lambda, k)\ \text{(MeV mb)}$$

(k photon momentum transfer, $E_x/\hbar c$), it is evident that the actual contribution depends on the excitation energy. Effectively the dependence does not scale with $E_x^{\,3}$ due to the effect of the energy weighted sum rule and the fact that k is no longer small. Since

$$B(E\lambda, k) = (2\lambda+1)\left|\frac{(2\lambda+1)!!}{k^\lambda}\int_0^\infty j_\lambda(kr)\rho_{\mathrm{tr}}(r)r^2 dr\right|^2$$

[which transfers into the familiar $(2\lambda+1)\,|\int_0^\infty \rho_{\mathrm{tr}}(r) r^{\lambda+2} dr|^2$ for $k\to 0$], $B(E\lambda,k)$ falls off with rising excitation energy. For example, $B(E2, k = 0.25) \approx 0.8\ B(E2,0)$. Table VII shows for ^{140}Ce some examples of possible contributions of $E2$ strength to the photon cross section in units of the Thomas-Reiche-Kuhn sum rule (TRK) under the assumptions specified in the caption.

A recent monochromatic (γ,n) measurement,[88] which extended an earlier one[59] to $E_\gamma = 100$ MeV, found for $^{\mathrm{nat}}$Ce the total cross section up to that energy to be 1.7×TRK. The cross section in excess of a Lorentz line extrapolation of the GDR at 15 MeV rises to approximately 8 mb at 55 MeV and stays relatively constant out to 100 MeV.[88]

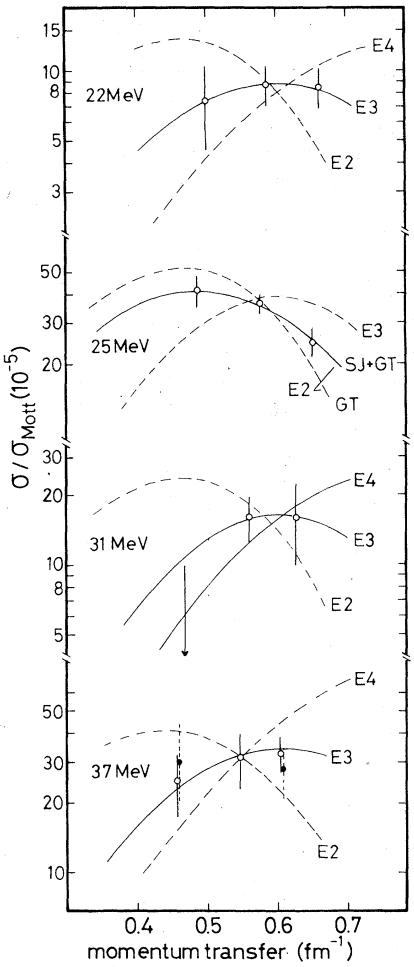

FIG. 10. Comparison of the DWBA and experimental form factors for the resonances found at 22, 25, 31, and 37 MeV. The Goldhaber-Teller model for an $E3$ transition fits the experimental form factors of the resonance found at 22 MeV. Both the Goldhaber-Teller and the Myers-Swiatecki $E2$ models were fit to the experimental form factors for the resonance found at 25 MeV (Table X). The Myers-Swiatecki model with a mixture ratio of 1.0 was found to fit the data better than the Goldhaber-Teller model as explained in the text. The assignment of an $E3$ transition can be clearly ruled out. The experimental form factor of the resonance found at 31 MeV fit the Goldhaber-Teller model for both $E3$ and $E4$ transition. An upper value could only be estimated for the form factor obtained from the 80 MeV/90° experiment, based on the statistical error of the measurement. The assignment of an $E2$ transition can be ruled out. The assignment of the resonance around 37 MeV is the most difficult. Because of the intricate arguments, we refer to the text.

Table VII shows that (1) the isovector $E2$ strength at 25 MeV (50% EWSR) already contributes 0.05 TRK to the total photon sum and (2) that the missing isoscalar (30% EWSR) and isovector (50% EWSR) $E2$ strength easily can contribute another 40–50% of the TRK sum rule between 50 and 100 MeV (see caption to Table VII). That means that in ^{140}Ce as well as in ^{28}Si all of the cross section in excess of the GGT sum rule could be (but does not necessarily have to be) of $E2$ nature. Since nothing in the derivation of the GGT sum rule limits the contributing multipolarities to $E1$, the fundamentally important discrepancy between experiment and the GGT sum rule still prevails.[89] But we think the actual nature and nuclear origin of the cross section up to the pion threshold merits more investigations. Perhaps future (e, e') coincidence experiments will shed some light on this question.

D. Octupole and Isovector monopole strength

In contrast to the quadrupole strength expected from the Bohr and Mottelson self-consistent shell model,[7,9,11] the octupole strength has been more elusive. This is understandable for once, because (Table I) there are two main shell transitions allowed by spin and parity, namely $1\hbar\omega$ and $3\hbar\omega$. Although many $E3$ states at $\sim 30A^{-1/3}$ MeV have been known from electron scattering in the $A \approx 50$ mass region since many years (see table 27 in Ref. 40), a systematic investigation has only recently been undertaken by Moss *et al.* with (α, α').[90] Although these states are below particle threshold, they are generally regarded as belonging to the giant resonance region and were called low energy octupole resonance (LEOR). The main feature of these high lying bound octupole state(s), HEBOS, as evolved from the (α, α') experiments in nuclei between ^{90}Zr and ^{154}Sm, is a concentra-

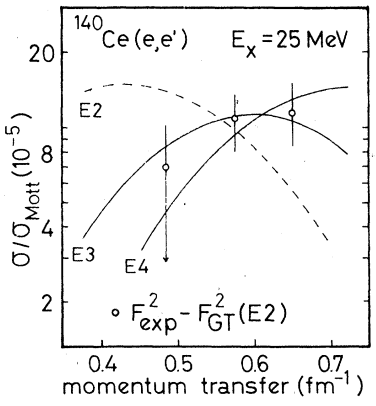

FIG. 11. Comparison of the difference between the experimental form factors and the Goldhaber-Teller model (see Fig. 11) to the DWBA form factor for the resonance found at 25 MeV. The difference shows that the possibility of an $E3$ or an $E4$ transition lying beneath the $E2$ transition exists if the Goldhaber-Teller model is assumed to be correct.

TABLE VII. Contribution of $E2$ strength to the photon cross section. For the calculation it was assumed that all the sum rule strength (isoscalar plus isovector = 1.14×10^5 MeV fm^4) would be distributed in the form of a Breit–Wigner curve with resonance maximum E_X and width Γ. The result is expressed in units of the classical sum rule (Ref. 85) and was calculated by integration from 10 MeV to 100 MeV and 140 MeV, respectively. To get possible contributions from $E2$ to the total photon cross section, σ_{100} (or σ_{140}) has to be multiplied by the sum rule fraction measured or assumed, and additionally by Z/A and N/A for isoscalar and isovector strength. For example, if we assume the 50% EWSR ($\Delta T = 1$) missing at 25 MeV to be localized at 60 MeV, with $\Gamma = 20$ MeV, $\sigma_{max} = 9$ mb, $\sigma_{100}^{int} = 12\%$ TRK, and $\sigma_{140}^{int} = 15\%$ TRK would result. While the assumption of Breit–Wigner form may not be justified, a constant $E2$ distribution with a width of 30 to 40 MeV at 60 to 80 MeV excitation energy would be in agreement with Ahrens *et al.* (Ref. 88) and contribute even more to the photon cross section (since the Breit–Wigner curve contains only 50% of the area within its halfwidth, assumption of a boxlike distribution would raise σ_{100}^{int} and σ_{100}^{int} by some 50 to 80% of its value, depending on location and width).

E_X (MeV)	Γ (MeV)	σ_{max} (mb)	σ_{100}^{int}/TRK	σ_{140}^{int}/TRK
12	2.8	12	0.06	0.08
25	6.5	21	0.16	0.18
25	13	10	0.20	0.24
40	15	21	0.29	0.34
60	20	30	0.42	0.50
	30	20	0.39	0.50
80	20	43	0.49	0.62
	30	29	0.43	0.60
	40	22	0.38	0.58

tion of many $E3$ levels in a relatively narrow range ($\Gamma \sim 2-3$ MeV), exhausting approximately 20% of the isoscalar EWSR in spherical nuclei, but much less in the deformed ^{154}Sm. The essential conclusions of Moss *et al.*[90] have been verified for a wider range of nuclei in a more extended survey by the same group,[91] covering 18 nuclei between ^{40}Ca and ^{208}Pb, with a notable weak strength in the double closed shell nucleus ^{40}Ca and a total absence in ^{208}Pb. Table VIII shows a comparison between nuclei for which results are available from both α and electron scattering. While there is some agreement for 3 nuclei, the α result for ^{208}Pb is in disagreement with Ziegler and Peterson,[73] who find 6% of the sum rule in one level at 5.6 MeV and perhaps 8% more in another one at 5.25 MeV.

In ^{140}Ce we were able to fit the HEBOS envelope with a Breit-Wigner shape of width $\Gamma = 1.7\pm0.2$ MeV at $E_x = 6$ MeV ($31A^{-1/3}$ MeV) and a strength of 19 ± 6 EWSR, which agrees with the (α,α') data for ^{142}Nd (see Table VIII). The topmost part of Fig. 12 shows this state to clearly follow an $E3$ form factor and Table VI shows that our result agrees also very well with the RPA calculations of Liu and Brown.[81] From Table I we learn finally

TABLE VIII. Comparison of $1\hbar\omega$ isoscalar octupole strength from (α,α') and (e,e').

Nucleus	E_X (MeV)	Method	R [a]	Ref.
^{58}Ni	~6.8 [b]	(α,α')	8 ± 2	91
^{58}Ni	6.95	(e,e')	13 ± 2	92
^{89}Y	7.1	(α,α')	$\sim20\pm5$	91
^{89}Y	7.4 [c]	(e,e')	12 ± 2 [c]	16
^{142}Nd	6.2	(α,α')	22 ± 6	91
^{140}Ce	6.0	(e,e')	19 ± 6	present work
^{208}Pb		(α,α')		91
^{208}Pb	~5.4	(e,e')	14 ± 5	73

[a] $E_X B(E3)/\mathrm{EWSR}(E3,\Delta T=0)\times100$.
[b] Three states at 6.07, 6.85, and 7.55 MeV.
[c] Two concentrations of strength at 6.75 and 8.05 MeV.

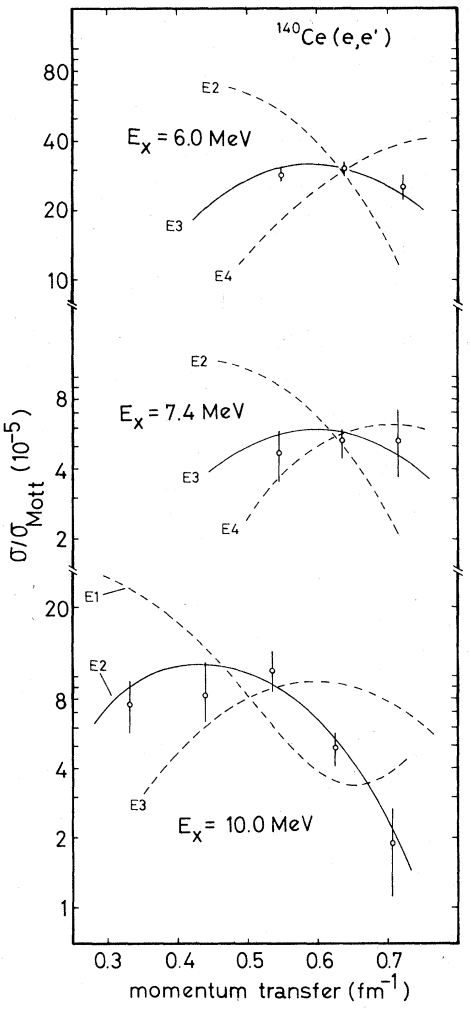

FIG. 12. Comparison of the DWBA and experimental form factors for the resonances found at 6.0, 7.4, and 10 MeV. The Goldhaber-Teller model for an $E3$ transition fits the experimental form factors of the 6.0 MeV resonance (Table X), while an $E2$ or $E4$ assignment of from factors can clearly be ruled out. The Goldhaber-Teller model for both an $E3$ and for an $E4$ transition fits the experimental form factors for the resonance found at 7.4MeV. An $E2$ assignment of the form factor, though, can be clearly ruled out. The Goldhaber-Teller model for an $E2$ ($E0$) transition fits the experimental form factors of the resonance found at 10 MeV, but the results depend on the interpretation of this mode (see Table V).

that together with the $E3$ state at 2.46 MeV (12 ± 2% EWSR, Ref. 2) all the strength expected from the schematic model for the $1\hbar\omega$ $E3$ transition (isoscalar) is exhausted.

The situation is more difficult for the higher $E3$ excitations. The isovector $1\hbar\omega$ $E3$ is expected to exhaust only a minor fraction of the sum rule (Table I) and can, therefore, probably not be distinguished in shape from the $E2$ resonance at 12 MeV. But this state may be partially responsible for the deviation of the measured 12 MeV cross section from the $E2$ form factor (Figs. 8 and 9).

The isoscalar $E3$ state is predicted to occur at ~105–115 $A^{-1/3}$ MeV (Table I, Table VI). Figure 1 shows, that indeed a resonance occurs in this energy region. It is also apparent from Fig. 1, that this mode will be difficult to measure because it is bracketed between the much stronger $E1$ at 15 MeV and the isovector $E2$ at 25 MeV. In addition, its strength may be fragmented, as indicated by the RPA calculations (Table VI) and the behavior of the resonance at 25 MeV discussed in Sec. IV C. Similar conclusions about the fragmentation have been drawn earlier for the closed shell nucleus ^{89}Y (Ref. 16). Despite these difficulties Figs. 3 and 5 show most clearly that cross section at 22 MeV becomes stronger with rising momentum transfer and is best described by an $E3$ form factor (Fig. 10). It has a width of 5 ± 1 MeV and exhausts (only) 19% of the EWSR, whereas the schematic model[10] predicts 72% and RPA calculations[81] 39%. But if we interpret the difference between experiment and the GT form factor for the 25 MeV resonance as $E3$, additional 20% strength are located in this region (Table VI).

The only nucleus where all the expected, octupole strength has been observed so far is ^{208}Pb (Ref. 4) where (90 ± 42)% EWSR has been reported. In ^{197}Au, within the same experiment,[4] only (45 ± 21)% were observed. This change in sum rule exhaustion does not necessarily mean that the strength is not there at all, it may just be differently distributed. The apparent greater dependence of the $E3$ strength on the (shell model) configuration of the nucleus gives hope that one will be able to learn more about nuclear structure from the octupole residual interaction than has been possible to date from the quadrupole. The very regular appearance of the latter does not reveal very much about the structure of the nucleus in which it occurs. This hope is especially justified for the HEBOS, since tthese states occur in the bound region of the excitation response.

The last member of the $E3$ continuum state family, the $3\hbar\omega$ isovector state is even more difficult to accurately determine. It is high in the continuum, i.e., it has presumably a large spreading width, and relatively small B values will exhaust considerable amounts of the sum rule. Consequently, one has to expect very small peak cross sections. The schematic model[10] predicts 195 $A^{-1/3}$ MeV (37–38 MeV in ^{140}Ce, Table I) which carries nearly all the isovector strength (97%). The RPA calculation[81] finds nearly the same amount centered at 36 MeV, with tails ranging

from 13 to 60 MeV. As Fig. 1 shows, there have been resonances seen in five nuclei heavier than ^{140}Ce [^{165}Ho (Ref. 71), ^{181}Ta (Ref. 72), ^{197}Au (Ref. 4), ^{208}Pb (Ref. 4), and ^{238}U (Ref. 93)]. The excitation energy scatters considerably in $A^{-1/3}$ units: thus, it is difficult to believe that this is the same state in all nuclei, and, in fact, the interpretation oscillates between $E0$ (isovector),[4] $E3$ (isovector),[71,93] and $E2+E4$ in Ref. 72. Although the ^{181}Ta experiment of Hicks *et al.*[72] is by far the best (e,e') measurement of any nucleus in the giant resonance region, what concerns statistical accuracy and momentum transfer covered, direct use of their data is hampered by the following. First, the angle was varied between 40° and 150°, giving rise to difficulties with transverse contributions (see discussion in Sec. IV B). Secondly, the authors did not use a strict hydrodynamical model ($c_{tr}/c = 1$, see above), but chose to generally fit the model to the data, making a direct comparison with their data impossible, with the exception of the $E2$, in which case the conversion factors can be extracted from Ref. 72. Our conclusion is, that their lower q data, which are also the more forward angle spectra, are compatible with $E3$ as well.

Since the isovector monopole has been predicted (Ref. 94, see caption of Table I for details) at 178 $A^{-1/3}$ MeV, the structure seen in this region may indeed be a mixture of both isovector monopole and $3\hbar\omega$ octupole. The scatter of excitation energy, in addition, can be explained consistently if we assume the higher resonance to be $E3$. Similar to the lower octupole states,[16,90-93] its strength might be spread out sufficiently in deformed nuclei as to disappear in the background (the spreading process presumably can be thought of as a quadrupole-octupole coupling). Therefore, in the deformed nuclei one sees the lower-lying monopole state, which in spherical nuclei cannot be recognized in resonant form because it is bracketed between the isovector $E2$ (135 $A^{-1/3}$ MeV) and the $E3$ (195 $A^{-1/3}$ MeV). While it should be clear that most of the interpretation given above is inferred from a skimpy data basis, it also might be pointed out that it is the only interpretation which is consistent with both theory and experiment.

In ^{140}Ce we have encountered the same ambiguities as apparent from the systematics in Fig. 1, amplified in our evaluation procedure through a chance happening in our experiment. In Sec. II we mentioned that the spectrum with the highest momentum transfer was measured twice in order to achieve sufficiently good statistical accuracy in a tolerable time ($\lesssim$ 100 h). In fact a machine failure of several hours duration in the first of the two runs produced an obviously unphysical discontinuity in the spectrum beyond 42 MeV. The 37 MeV state form factor in Fig. 10 shows two sets of points. The filled circles, favoring an $E2$ (or $E0$) form factor, correspond to a fit of the composite spectra up to 42 MeV. The open circles, favoring an $E3$ interpretation, correspond to a fit to the second run only, but up to 48 MeV in excitation energy. Correspondingly, the apparent maximum shifted from 37 to 38 MeV (~$195A^{-1/3}$ MeV) to 34 MeV ($175A^{-1/3}$ MeV). This is evident in Fig. 5, where the lower spectrum clearly shows that the resonance at the highest excitation energy (fixed at 37 MeV) does not describe the data very well; a relative maximum appears to be at 34 MeV. Our interpretation is that the χ^2 fit, attempting to achieve the lowest possible χ^2 (per degree of freedom) mismatches the background, verifying our rule of thumb, that in order to fit the continuum resonances reliably the spectra have to extend at least one full half-width beyond the last resonance fitted. Naturally, it would be possible to insert two resonances in this region one at 34 and one at 37 MeV, and attempt to disentangle the spectra that way. However, to do so would pretend that a greater accuracy is achievable, than justified by the data basis and our method of fitting the background together with the resonances. The latter obviously leads to difficulties at high excitation energies. The values given in Table X for the 34–38 MeV region thus should be interpreted as upper limits with any mixture of monopole and octupole possible. Within the errors both microscopic[81]

TABLE IX. Known $E4$ (isoscalar?) continuum excitations.

^{58}Ni [a]			^{60}Ni [a]			^{140}Ce		
E_X (MeV)	E_X ($A^{-1/3}$ MeV)	R [b]	E_X (MeV)	E_X ($A^{-1/3}$ MeV)	R [b]	E_X (MeV)	E_X ($A^{-1/3}$ MeV)	R [b]
9.6	37	5 ± 2	11.4	43	3 ± 2	7.4	38	7 ± 3
15.1	58	40 ± 15	14.9	58	20 ± 10	~12 [c]	~ 62 [c]	20 ± 10 [c]
						~25 [c]	~130 [c]	60 ± 30 [c]
			40	157	150 ± 75	31	161	80 ± 40

[a]Reference 92.

[b]$R = E_X B(E4)/\mathrm{EWSR}(E4, \Delta T = 0)$.

[c]Inferred from difference to $E2$ form factor.

and macroscopic[10,94] predictions can be accommodated.

E. Hexadecapole strength

There has been little convincing evidence for $E4$ excitations into the continuum. Similar to the $E3$ states, they are fragmented into four transitions ($2\hbar\omega$, $4\hbar\omega$, and these into isoscalar and isovector), and since they are even higher in excitation energy, they will be more spread out and smaller cross sections will exhaust the sum rule. As outlined earlier, to determine a certain multipolarity with certainty, on the basis of the form factor alone, one has to have a momentum transfer which covers the maximum of the form factor. This is not the case for the $E4$. However, for the states believed to be $E4$ a classification with $\lambda > 4$ would lead to multiple exhaustion of the sum rule. Table IV shows the results from our laboratory for ^{58,60}Ni (Ref. 92) and ^{140}Ce. For the Ni isotopes a line shape fit for all the $E4$ contributions was possible; in ^{140}Ce, as already discussed, some are inferred from differences to form factors and thus might be due to failures of models. The table shows a certain regularity concerning strength and position (in $A^{-1/3}$ MeV), surprising for nuclei that far apart in the nuclear system. Comparison with Table I shows some agreement with the schematic model prediction for both isoscalar $2\hbar\omega$ and $4\hbar\omega$ transitions what concerns the excitation energy, but clearly more work and better data are needed to establish a systematic behavior. The states at 7.4 MeV and 31 MeV, however, could be fitted by a line shape; Figs. 12 and 10, respectively, show that an $E4$ assignment is favored by the form factor.

It is clear that the sum rule would be approximately exhausted by a factor of two if all the states in Table IX indeed would be $E4$. Figure 9 shows for the 12 MeV region that $E3$ is favored in explaining the difference in cross section to the GT $E2$ DWBA calculation (Fig. 8); for the 25 MeV region (Fig. 10) we have argued above that one would not expect the Goldhaber-Teller model to fit the isovector $E2$. That means, together with the 2.08 MeV state (4% EWSR, Ref. 2), some 90% of the isoscalar sum are exhausted, but the distribution seems to be different than predicted by the schematic model,[10] or the microscopic calculations.[81] However, the large uncertainties preclude definite conclusions.

F. The 53 $A^{-1/3}$ MeV state

All the results discussed so far have been categorized according to certain multipolarities and straight forward macroscopic and microscopic considerations. The 53 $A^{-1/3}$ MeV (10 MeV) state defies such treatment. Discovered in the experiments described in Refs. 2 and 3, correctly recognized as electric in character, its systematic occurrence was first verified by (e,e') on ^{197}An and ^{208}Pb.[4] Although Ref. 2 does not give a multipolarity, it is clear from the spectra that it scales with the GQR at 12 MeV. Consequently, it was a natural candidate for a monopole assignment.[4] Since this assignment in ^{208}Pb was based on some intricate argument concerning fine structure in both (γ,n) and (e,e'), it was argued it might as well be quadrupole,[76] or the monopole assignment was even ruled out.[95] Since we did not agree with this conclusion, we have given a detailed account of history and arguments recently,[69] to which we refer for particulars. There are two new elements which make it possible and necessary to amend the statement in the abstract of Ref. 69 that "the new analysis makes any assignment for the 8.9 MeV resonance other than monopole difficult to understand." Despite that sentence, arguments in favor of an isovector $E2$ resonance were given,[69] and understood.[96]

The two new elements are:

1. A ^{207}Pb (n,γ) experiment by Raman *et al.*[96] shows, based on the technique developed in Ref. 17, that the 8.9 MeV resonance in ^{208}Pb has to be $E2$ in order to explain the slope of primary $E2$ transitions (monopole states decay only in higher order through γ emission).

2. The availability of more (e,e') data for the 53 $A^{-1/3}$ MeV region in a number of nuclei between ^{58}Ni and ^{208}Pb. The systematics of this resonance is indeed different from any other electric resonance found so far. Generally, the strength of giant resonances varies very slowly with A, dropping from approximately 80 to 100% EWSR for the isoscalar GQR in the heaviest nuclei, to 50 to 60% in the $A \approx 60$ region.[12,13] This is quite different for the $53A^{-1/3}$ MeV state. If we express its strength in units of the isoscalar $E2$ sum rule, because it undoubtedly follows an $E2$ (or $E0$) form factor, its strength drops from 35% in ^{208}Pb (Refs. 4, 69, 76) to 9% in ^{140}Ce and below 3% in ^{58}Ni. Figure 12 shows that an $E2$ (or $E0$) form factor explains the ^{140}Ce data best.

There are many possibilities to display the strength of the $53A^{-1/3}$ MeV resonance as a function of various parameters. The one which produced the greatest consistency is shown in Fig. 13 and displays the isovector $E2$ strength as function of the neutron excess. Clearly, the strength rises in proportion to T^2. The most important case is ^{208}Pb. Not only has this state been measured by several experiments, or different evaluation of the

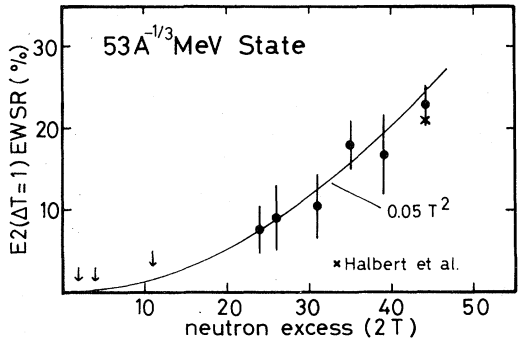

FIG. 13. Strength of state at $53\,A^{-1/3}$ MeV in nuclei between ^{58}Ni and ^{208}Pb expressed in units of the isovector sum rule. The calculation of Halbert *et al.* (Ref. 82), normalized to the strength found experimentally for the isoscalar $E2$ in ^{208}Pb (92% EWSR), is indicated. The experimental points are from Ref. 92 (^{58,60}Ni), Ref. 16 (^{89}Y), this work (^{140}Ce), Ref. 29 (^{142}Nd), Ref. 71 (^{165}Ho), average of Ref. 20 and Ref. 72 (which had to be renormalized, see discussion in connection with the 37 MeV resonance) (^{181}Ta), Ref. 4 (^{197}Au), and the average of Ref. 4, 69, 76, and 97 (^{208}Pb). For the three lightest nuclei only upper limits for the $E2$ strength can be given. A resonance with a width of 1–2 MeV in the Ni isotopes at this energy is predominantly $E3$, in ^{89}Y no resonant cross section could be identified at all.

same data have been made,[4,69,76,96,97] it is also the only case where applicable RPA calculations have been performed.[82] Halbert *et al.*[82] have calculated with RPA wave functions that the $T=1$ and $T=0$ sums in the region of the isoscalar giant quadrupole resonance in ^{208}Pb should be in the ratio 0.23.

Figure 13 shows this calculation to be in close agreement with the strength of the $53A^{-1/3}$ MeV state. From the context of the discussion in Ref. 82, it appears that this strength is thought to be due to the excess neutrons, although a simple mass oscillation model would only produce isovector strength of the order $(N-Z)^2/A^2$, or $\frac{1}{5}$ of the microscopic result.[82] Similar considerations by Bohr and Mottelson (Ref. 11, page 513) must not be interpreted as suggesting a special mode of oscillation associated with the excess neutrons,[98] because it would be difficult to imagine a force which holds together the excess neutrons in a separate oscillation against the rest of the nucleus.[98] On the other hand, it seems clear from the experimental evidence (see discussion in Ref. 69, especially the apparent nonexcitation in hadron scattering) that this mode is not just a simple sec-

TABLE X. Results in units of the reduced transition probabilities (B values), ground state radiation width (Γ_γ^0), and energy weighted sum rule exhaustion, for the major resonances found in this experiment. Some results for weaker states, and those inferred from differences between cross sections and DWBA calculation, are, together with the appropriate discussion, scattered in the text. The isospin assignments are not determined by this experiment, but were taken from comparison with other experiments and theory.

E_X (MeV)	$E_X A^{-1/3}$ (MeV)	Γ (MeV)	$E\lambda$	ΔT	$B_{\rm exp}$ (fm$^{2\lambda}$) [a]	Γ_γ^0 (eV)	R [b]	Std. [c] dev.	Total [d] error
6.0 ± 0.2	31	1.7 ± 0.2	3	0	1.3×10^5	2.0×10^{-3}	19	± 3	± 6
10.0 ± 0.2	52	1.8 ± 0.2	2	0	430	7.6	9	± 2	± 4
			0	0	770		13	± 2	± 6
12.0 ± 0.2	62	2.8 ± 0.2	2	0	2.5×10^3	10.0	63 [e]	±17	±13
			2	0	2.0×10^3	8.7	50 [f]	± 5	±10
15.3 ± 0.2	79	4.4 ± 0.2	1	1	41	5.1×10^4	122 [g]	±12	±20
			1	1	55	6.9×10^4	167 [h]	±40	±27
22 ± 1	114	5 ± 1	3	0	3.7×10^4	4.9	19	± 2	±10
25 ± 1	130	6.5 ± 1	2	1	1.3×10^3	2.1×10^3	50 [i]	± 8	±15
			2	1	2.1×10^3	3.3×10^3	77 [h]	±25	±23
34 – 38	175	7 –10	3	0	1.2×10^5	6.8×10^2	75	±10	$\pm^{50}_{25}$
	195		0	1	2.8×10^3		130	±20	$\pm^{90}_{45}$

[a] For the monopole the measured quantity is $|M_{\rm if}|^2$ (fm^4).

[b] $R = E_X B(E\lambda)/\mathrm{EWSR}(E\lambda, \Delta T) \times 100$.

[c] The error given (in units of R) is the standard deviation of the average sum rule exhaustion and is, therefore, more a measure for the fit to a certain model than a measure for the total uncertainty.

[d] The total error (in units of R) is based on the maximum and minimum values found for the areas under the curves during the many attempts to fit the spectra.

[e] $c_{\rm tr} = 1.0c$.

[f] $c_{\rm tr} = 0.95c$.

[g] MS model with $\alpha = 0.76$.

[h] GT model.

[i] MS model with $\alpha = 1.0$.

ond branch of the GQR at 12 ($63A^{-1/3}$) MeV. Despite the objections raised, the explanation as a separate excess neutron isovector $E2$ shape oscillation seems to be the only one which explains all the data in a consistent manner.

V. SUMMARY

This work covers a large range of the nuclear continuum, which contains many resonances. Since they have been discussed in detail, often with complicated arguments, in the text, we do not want to give a short version of our paper here, open to misinterpretation. For a short overview concerning the major resonances, Table X may be consulted. Rather, we want to state the shortcomings. We have measured ^{140}Ce up to 48 MeV in excitation energy. The full use of the data has been hampered by two problems.

First, the continuum states are wide and overlap and are, therefore, difficult to disentangle with the overlapping resonances. This difficulty is a principal one and cannot be helped. Coincidence experiments are sometimes proposed as a remedy, but they do not measure the total cross section, and, as additional difficulty, will produce interference between resonances of different multipolarity.[40]

Secondly, the radiation tail fails at higher excitation energy, where those resonances lie which are open mainly to investigation by (e,e') (the isovector states). Little theoretical progress has been made here since the pioneering work of Refs. 27 and 30. Experimenters have made some heuristical improvements, first by inserting correct elastic cross sections into the peaking approximation,[73] and then by extending this method[32] to the formalism of Ginsberg and Pratt.[30] A greater theoretical effort to overcome this problem is clearly needed.

Coincidence experiments may be, however, the only method to decide whether or not the total photon cross section below pion threshold contains a large $E2$ contribution, or not. From our experiment we can only show that it might be possible.

If the 10 MeV state ($53A^{-1/3}$ MeV) is indeed a neutron oscillation, coincidence experiments may also help here. On the other hand, they may not, because neutrons are the only particles which come out of the nucleus at this excitation energy in heavy nuclei anyhow.

ACKNOWLEDGMENT

This research was supported in part by the National Science Foundation and the Naval Postgraduate School Research Foundation.

[1]S. S. Hanna, in *Proceedings of the International School on Electro- and Photonuclear Reactions*, edited by S. Costa and C. Scharf, published in "Lecture Notes in Physics," Vol. 61 (Springer, New York, 1977).
[2]Rainer Pitthan, Z. Phys. 260, 283 (1973).
[3]R. Pitthan and Th. Walcher, Phys. Lett. 36B, 563 (1971); Z. Naturforsch. 27a, 1683 (1972).
[4]R. Pitthan, F. R. Buskirk, E. B. Dally, J. N. Dyer, and X. K. Maruyama, Phys. Rev. Lett. 33, 849 (1974); 34, 848 (1975).
[5]O. Hansen and O. Nathan, Comments Nucl. Part. Phys. 5, 165 (1972).
[6]M. Danos, Ann. Phys. (Leipzig) 10, 18 (1952).
[7]Ben Mottelson, Nobel Prize Talk, Fys. Tidsskr. 74, 97 (1976); Rev. Mod. Phys. 48, 375 (1976); Science 193, 287 (1976).
[8]G. E. Brown and M. Bolsterli, Phys. Rev. Lett. 3, 472 (1959); G. E. Brown, L. Castillejo, and J. A. Evans, Nucl. Phys. 22, 1 (1961).
[9]B. R. Mottelson, in *Proceedings of the International Conference on Nuclear Structure, Kingston, 1960,* edited by D. A. Bromley and E. W. Vogt (Univ. of Toronto Press, Toronto/North-Holland, Amsterdam, 1960); A. Bohr, in *Nuclear Physics; An International Conference*, edited by R. Becker, C. Goodman, P. Stelson, and A. Zucker (Academic, New York, 1967).
[10]I. Hamamoto, in *Proceedings of the International Conference on Nuclear Structure Studies Using Electron Scattering and Photoreaction, Sendai, 1972,* edited by K. Shoda and H. Ui [Suppl. Res. Rep. Nucl. Sci., Tohoku Univ., 5, 205 (1972)].
[11]A. Bohr and B. R. Mottelson, *Nuclear Structure* (Benjamin, Reading, Mass., 1975), Vol. II.
[12]R. Pitthan, Phys. Rep. (to be published).
[13]D. H. Youngblood, J. M. Moss, C. M. Rozsa, J. D. Bronson, A. D. Bacher, and D. R. Brown, Phys. Rev. C 13, 994 (1976).
[14]J. M. Moss, Bull. Am. Phys. Soc. 22, 574 (1977).
[15]Yung-Su Tsai, Rev. Mod. Phys. 46, 815 (1974).
[16]R. Pitthan, F. R. Buskirk, E. B. Dally, J. O. Shannon, and W. H. Smith, Phys. Rev. C 16, 970 (1977).
[17]E. F. Gordon and R. Pitthan, Nucl. Instrum. Methods 145, 569 (1977).
[18]F. E. Bertrand, Annu. Rev. Nucl. Sci. 26, 457 (1976).
[19]D. H. Youngblood, C. M. Rosza, J. M. Moss, D. R. Brown, and J. D. Bronson, Phys. Rev. Lett. 39, 1188 (1977).
[20]H. Miura and Y. Torizuka, Phys. Rev. C 16, 1688 (1977).
[21]A. Richter, in *Proceedings of the Sendai Conference on Electro- and Photoexcitations*, Sendai 1977 [Res. Report. Lab. Nucl. Science, Tohoku Univ. 10, (Suppl.) 195 (1977)].
[22]J. Schwinger, Phys. Rev. 76, 760 (1949).
[23]W. C. Barber, F. Berthold, G. Fricke, and F. E. Gudden, Phys. Rev. 120, 2081 (1960).
[24]L. C. Maximon, Rev. Mod. Phys. 41, 193 (1969).
[25]L. W. Mo and Y. S. Tsai, Rev. Mod. Phys. 41, 205 (1969).
[26]Y. S. Tsai, in *Nuclear Structure*, edited by R. Hof-

stadter and L. I. Schiff (Stanford Univ. Press, Stanford, Calif., 1964), p. 221.
[27]L. C. Maximon and D. B. Isabelle, Phys. Rev. 136, B674 (1964).
[28]Leonard C. Maximon, NBS Technical Note No. 955, 1977 (unpublished).
[29]A. Schwierczinski, Dissertation, Technische Hochschule Darmstadt, 1976 (unpublished).
[30]E. S. Ginsberg and R. H. Pratt, Phys. Rev. 134, B773 (1964).
[31]Yung-Su Tsai, SLAC Report No. SLAC-PUB-848, 1971 (unpublished).
[32]F. R. Buskirk, H. D. Gräf, R. Pitthan, H. Theissen, O. Titze, and Th. Walcher, Phys. Lett. 42B, 194 (1972).
[33]T. de Forest and J. D. Walecka, Adv. Phys. 15, 1 (1966).
[34]A. Migdal, J. Phys. USSR 8, 331 (1944).
[35]W. Bothe and W. Gentner, Z. Phys. 106, 263 (1937); 112, 45 (1939).
[36]H. Bethe and R. Bacher, Rev. Mod. Phys. 8, 82 (1936).
[37]M. Goldhaber and E. Teller, Phys. Rev. 74, 1046 (1948).
[38]H. Steinwedel and H. Jensen, Z. Naturforsch. 5a, 413 (1950).
[39]B. L. Berman and S. C. Fultz, Rev. Mod. Phys. 47, 713 (1975).
[40]H. Überall, *Electron Scattering from Complex Nuclei* (Academic, New York 1971).
[41]W. D. Myers, W. J. Swiatecki, T. Kodama, L. J. El-Jaick, and E. R. Hilf, Phys. Rev. C 15, 2032 (1977).
[42]W. D. Myers and W. J. Swiatecki, Ann. Phys. (N.Y.) 55, 395 (1969).
[43]N. Marty, M. Morlet, A. Willis, V. Comparat, and R. Frascaria, in *Proceedings of the International Symposium on Highly Excited States in Nuclei, Jülich, 1975,* edited by A. Faessler, C. Mayer-Böricke, and P. Turek (KFA Jülich, W. Germany, 1975).
[44]D. H. Youngblood, C. M. Rosza, J. M. Moss, D. R. Brown, and J. D. Bronson, Phys. Rev. Lett. 39, 1188 (1977).
[45]L. Meyer-Schützmeister, Z. Vager, R. E. Segel, and P. P. Singh, Nucl. Phys. A108, 180 (1968).
[46]C. -P. Wu, F. W. K. Firk, and T. W. Phillips, Nucl. Phys. A147, 19 (1970).
[47]R. B. Watson, D. Branford, J. L. Black, and W. J. Caelli, Nucl. Phys. A203, 209 (1973).
[48]G. S. Foote, D. Branford, D. C. Weisser, N. Shikazono, R. A. I. Bell, and F. C. P. Huang, Nucl. Phys. A263, 349 (1976).
[49]S. Fukuda and Y. Torizuka, Phys. Lett. 62B, 146 (1976). An earlier account of these data, with differing results, appeared in Phys. Rev. Lett. 29, 1109 (1972).
[50]Mamiko Sasao and Y. Torizuka, Phys. Rev. C 15, 217 (1976).
[51]A. Richter, Contributed paper to the IVth Seminar on Electromagnetic Interactions of Nuclei at Low and Medium Energies, Moscow, 1977 (unpublished).
[52]S. T. Tuan, L. E. Wright, and D. S. Onley, Nucl. Instrum. Methods 60, 70 (1968).
[53]N. Glossmann and C. Toepffer, Nucl. Phys. A161, 330 (1971).
[54]R. Pitthan, Dissertation, Technische Hochschule Darmstadt, 1972 (unpublished).
[55]D. S. Onley and D. L. Wright 1978 (unpublished).
[56]R. Pitthan, Laboratory Report No. 44, Institut für Technische Kernphysik, Technische Hochschule Darmstadt, 1971 (unpublished).
[57]Y. Kawazoe, Res. Rep. Lab. Nucl. Sci. Tohoku Univ. 6, 211 (1973).
[58]D. G. Ravenhall, D. R. Yennie, and R. N. Wilson, Phys. Rev. 95, 500 (1964).
[59]A. Leprêtre H. Beil, R. Bergère, P. Carlos, J. Fagot, A. de Miniac, A. Veyssière, and H. Miyase, Nucl. Phys. A258, 350 (1976).
[60]Z. M. Szalata, K. Itoh, G. A. Peterson, J. Flanz, S. P. Fivozinsky, F. J. Kline, J. W. Lightbody, X. K. Maruyama, and S. Penner, Phys. Rev. C 17, 435 (1978).
[61]B. L. Berman, Lawrence Livermore Laboratory Report No. UCRL-78482, 1976 (unpublished).
[62]A. Schwierczinski, R. Frey, E. Spamer, H. Theissen, and Th. Walcher, Phys. Lett. 55B, 171 (1975).
[63]Th. H. Schucan, Nucl. Phys. 61, 417 (1965).
[64]G. R. Satchler, Part. Nucl. 5, 105 (1973).
[65]M. N. Harakeh, K. Van der Borg, T. Ishimatsu, H. P. Morsch, A. Van der Woude, and F. E. Bertrand, Phys. Rev. Lett. 38, 75 (1977).
[66]A. Goldmann, Z. Phys. 234, 144 (1970).
[67]F. H. Lewis and J. D. Walecka, Phys. Rev. 133, B849 (1964).
[68]P. Paul, in *Proceedings of the International Symposium on Highly Excited States in Nuclei, Jülich, 1975,* Ref. 43, Vol. 2.
[69]R. Pitthan and F. R. Buskirk, Phys. Rev. C 16, 983 (1977).
[70]A. Richter, Ref. 1.
[71]G. L. Moore, F. R. Buskirk, E. B. Dally, J. N. Dyer, X. K. Maruyama and R. Pitthan, Z. Naturforsch. 31a, 668 (1976).
[72]R. S. Hicks, I. P. Auer, J. C. Bergstrom, and H. S. Caplan, Nucl. Phys. A278, 261 (1977).
[73]J. F. Ziegler and G. A. Peterson, Phys. Rev. 165, 1337 (1968).
[74]G. F. Bertsch and S. F. Tsai, Phys. Rep. 18C, 126 (1975).
[75]T. J. Deal and S. Fallieros, Phys. Rev. C 7, 1709 (1973).
[76]A. Schwierczinski, R. Frey, A. Richter, E. Spamer, H. Theissen, O. Titze, Th. Walcher, S. Krewald, and S. Rosenfelder, Phys. Rev. Lett. 35, 1244 (1975).
[77]S. P. Kamerdzhiev, Yad. Fiz. 15, 676 (1972)[Sov. J. Nucl. Phys. 15, 379 (1972)].
[78]S. P. Kamerdzhiev, Phys. Lett. 47B, 147 (1973).
[79]P. Ring and J. Speth, Phys. Lett. 44B, 477 (1973).
[80]G. F. Bertsch, Phys. Rev. Lett. 31, 121 (1973).
[81]K. F. Liu and G. E. Brown, Nucl. Phys. A265, 385 (1976).
[82]E. C. Halbert, J. B. McGrory, G. R. Satchler, and J. Speth, Nucl. Phys. A245, 189 (1975).
[83]J. Ahrens, H. Borchert, K. H. Czock, H. B. Eppler, H. Gimm, H. Gundrum, M. Kröning, P. Riehn, G. Sita Ram, A. Zieger, and B. Ziegler, Nucl. Phys. A251, 479 (1975).
[84]R. Pitthan, F. R. Buskirk, J. N. Dyer, E. E. Hunter, and G. Pozinsky, Phys. Rev. C 19, 299 (1979).
[85]W. Thomas, Naturwissenschaften 13, 627 (1923); F. Reiche and W. Thomas, Z. Phys. 34, 510 (1925); W. Kuhn, *ibid.* 33, 408 (1925).
[86]*Photonuclear Reactions*, Benchmark Papers in Nuclear Physics, edited by E. G. Fuller and E. Hayward (Dowden, Hutchington and Ross, Stroudsburg, Pennsylvania, 1976), p. 391.
[87]M. Gell-Mann, M. L. Goldberger, and W. E. Thirring, Phys. Rev. 95, 1612 (1954).
[88]J. Ahrens, H. Beil, R. Bergere, P. Carlos, P. Daujat, J. Fagot, P. Garganne, U. Kneissl, A. Leprêtre, A. de Miniac, and A. Veyssière, Compte Rendu d'Activité, 1976-1977, CEN Saclay, France, report (unpub-

lished), p. 71.
[89]W. Weise, Phys. Rep. 13C, 54 (1974).
[90]J. M. Moss, D. H. Youngblood, C. M. Rosza, D. R. Brown, and J. D. Bronson, Phys. Rev. Lett. 37, 816 (1976).
[91]J. M. Moss, D. R. Brown, D. H. Youngblood, C. M. Rosza, and J. D. Bronson, Phys. Rev. C 18, 741 (1978).
[92]R. Pitthan, G. M. Bates, J. S. Beachy, F. R. Buskirk, E. B. Dally, D. H. Dubois, J. N. Dyer and S. J. Kowalick, Phys. Rev. C (to be published).
[93]W. A. Haouk, R. W. Moore, F. R. Buskirk, J. N. Dyer, and R. Pitthan, Bull. Am. Phys. Soc. 22, 542 (1977); and to be published.
[94]T. Suzuki, Nucl. Phys. A217, 182 (1973).
[95]F. E. Bertrand and D. C. Kocher, Phys. Rev. C 13, 2241 (1976).
[96]S. Raman, M. Mizumoto, G. G. Slaughter, and R. L. Macklin, Phys. Rev. Lett. 40, 1306 (1978).
[97]M. Nagao and Y. Torizuka, Phys. Rev. Lett. 30, 1068 (1973).
[98]A. Bohr and B. R. Mottelson, private communication.